GeoArabia, Vol. 9, No. 4, 2004
Gulf Petrolink, Bahrain

Petroleum generation and migration in the Mesopotamian Basin and Zagros Fold Belt of Iraq: results from a basin-modeling study

Janet K. Pitman, Douglas Steinshouer, and Michael D. Lewan

ABSTRACT

A regional 3-D total petroleum-system model was developed to evaluate petroleum generation and migration histories in the Mesopotamian Basin and Zagros fold belt in Iraq. The modeling was undertaken in conjunction with Middle East petroleum assessment studies conducted by the USGS. Regional structure maps, isopach and facies maps, and thermal maturity data were used as input to the model. The oil-generation potential of Jurassic source-rocks, the principal known source of the petroleum in Jurassic, Cretaceous, and Tertiary reservoirs in these regions, was modeled using hydrous pyrolysis (Type II-S) kerogen kinetics. Results showed that oil generation in source rocks commenced in the Late Cretaceous in intrashelf basins, peak expulsion took place in the late Miocene and Pliocene when these depocenters had expanded along the Zagros foredeep trend, and generation ended in the Holocene when deposition in the foredeep ceased. The model indicates that, at present, the majority of Jurassic source rocks in Iraq have reached or exceeded peak oil generation and most rocks have completed oil generation and expulsion. Flow-path simulations demonstrate that virtually all oil and gas fields in the Mesopotamian Basin and Zagros fold belt overlie mature Jurassic source rocks (vertical migration dominated) and are situated on, or close to, modeled migration pathways. Fields closest to modeled pathways associated with source rocks in local intrashelf basins were charged earliest from Late Cretaceous through the middle Miocene, and other fields filled later when compression-related traps were being formed. Model results confirm petroleum migration along major, northwest-trending folds and faults, and oil migration loss at the surface.

INTRODUCTION

Iraq is a major petroleum-producing country in the Middle East (Figure 1), with current proven reserves of 113 billion barrels of oil (BBO) and 110 trillion cubic feet (TCF) of gas in three total petroleum systems (see inset map on Figure 1 for names and locations) (USGS, 2000; Ahlbrandt et al., 2000; Verma et al., 2004). Total undiscovered oil resources in these total petroleum systems, exclusive of reserve growth, are estimated to be between 14 and 84 billion barrels (5% and 95% probability range), with a mean value of 45 billion barrels (Ahlbrandt et al., 2000; Verma et al., 2004). A discussion of reserve growth in discovered fields and a summary of recoverable and proved oil and gas reserves by field, including oil properties are presented in Verma et al. (2004). Most of the petroleum that has been discovered in Iraq is reported to have been sourced from Jurassic rocks and trapped in Cretaceous and Tertiary reservoirs in the Mesopotamian Basin and Zagros fold belt (Figure 1). The USGS developed a regional total petroleum-system model of the stratigraphic section hosting these source rocks and reservoirs to: (1) define the level and extent of source-rock maturity; (2) establish the temperature and timing of important petroleum generation events, and (3) identify the migration pathways that charged major oil and gas fields. Earlier versions of this model were used to evaluate the source-rock generation potential of undrilled prospects in these regions (see Verma et al., 2004).

Historically, it has been difficult to assess petroleum resources in the Mesopotamian Basin and Zagros fold belt because data on the source rocks and reservoir rocks have not been available. Several studies document the stratigraphy and sedimentology of Jurassic source rocks (Sadooni, 1997; Alsharhan and Nairn, 1997, Sadooni and Aqrawi, 2000; Sharland et al., 2001), and burial-temperature histories have been published for a few wells (Ibrahim, 1983); however, a regional analysis of source-rock maturation is unavailable, and the timing and extent of oil generation, and secondary migration have not been adequately addressed.

Basin modeling provides insights into total petroleum-system processes, which can optimize resource assessments and exploration efforts in under-explored basins. Basin-model simulations take into account interpretations gained from geologic models and are based on knowledge of the source

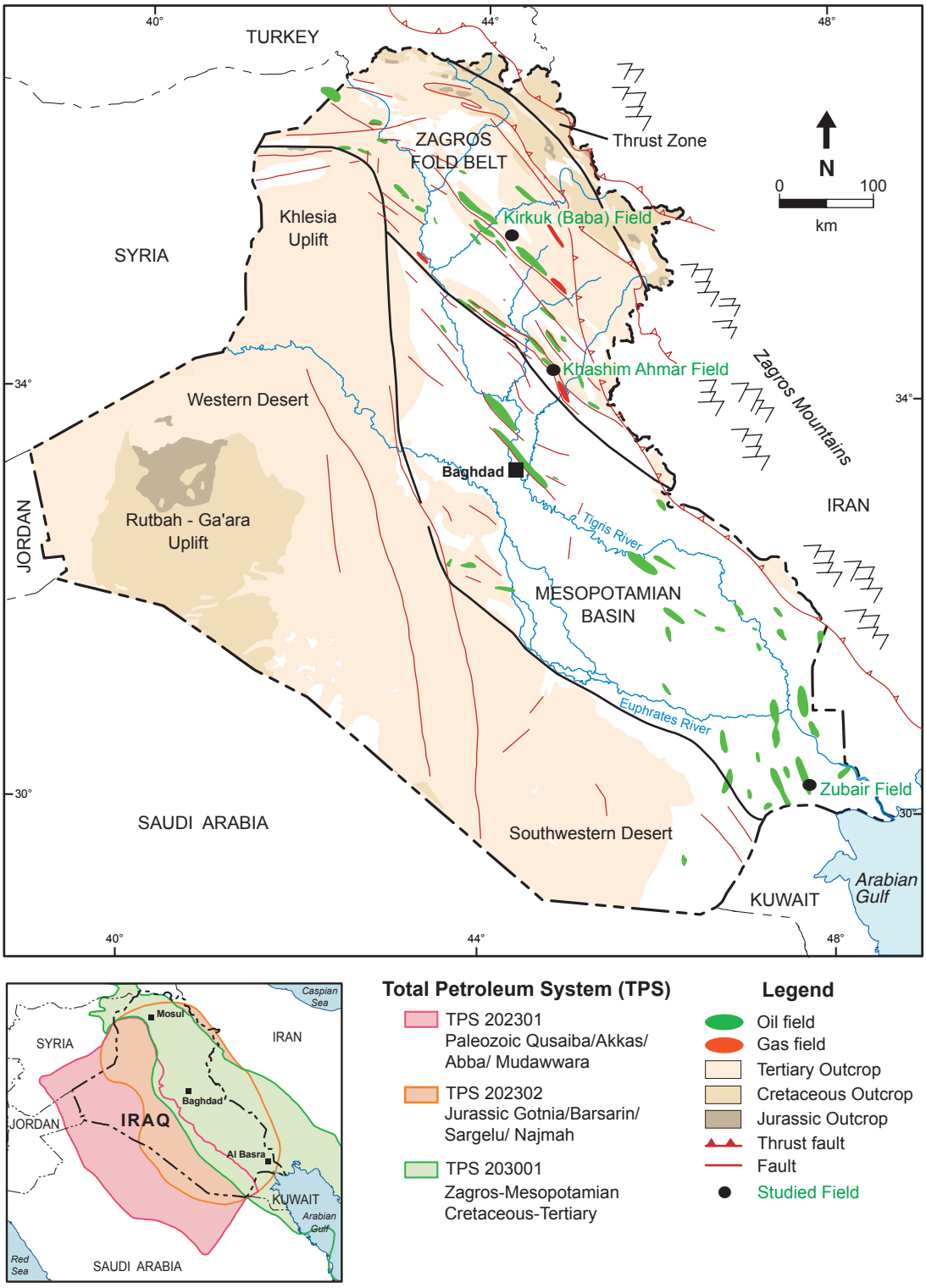

Figure 1: Map showing location of Mesopotamian Basin and Zagros fold belt, and major oil and gas fields in these regions (modified from Aqrawi, 1998). Inset map depicts three Total Petroleum Systems (TPS) that have contributed to the petroleum accumulations in Iraq (Ahlbrandt et al., 2000). Zubair, Khashim Ahmar, and Kirkuk fields were selected for 1-D modeling.

rock, reservoir rock, traps, and seals in the total petroleum system. A regional, three-dimensional, total petroleum-system model of Iraq was developed using Integrated Exploration System (IES) Petromod software (Note: use of brand name is for descriptive purposes only and does not constitute endorsement by the U.S. Geological Survey). Petromod is a finite-element, basin simulator that describes thermal histories, source rock maturity, and petroleum generation and migration in one, two,

and three dimensions (1-D, 2-D, and 3-D, respectively) (IES, 2004). The generalized nature of the input data and the lack of adequate data for model calibration precluded analysis of 3-D model results on a field-by-field basis; however, on a regional scale, the 3-D model provided valuable insights into timing of petroleum generation and migration and directions of petroleum flow. Results and interpretations from petroleum-system models were utilized in the USGS (2000) World Petroleum Assessment.

GEOLOGIC SETTING

The Mesopotamian Basin forms a narrow belt that extends from northern Iraq to the Arabian Gulf (Figure 1). In Iraq, the basin is bounded on the east by the Zagros Mountains and on the west by the Mesozoic stable shelf. To the northwest, the basin converges with the Zagros fold belt, which extends along the Zagros orogenic front. The term Zagros fold belt, as used in this paper, corresponds to the Mesopotamian foredeep (Geosynclinal flank) and central faulting zones, as defined by Ditmar et al. (1972, unpublished report).

The Mesopotamian Basin originated as a NW-trending foredeep that formed in response to the continental collision of the Arabian Plate and continental blocks of Eurasia during the Late Cretaceous (Ameen, 1992; Beydoun, 1993; Beydoun et al., 1992). Throughout most of the Paleogene (early Tertiary), plate-margin deformation decreased, but in the late Paleogene and Neogene (middle to late Tertiary), continental convergence was renewed culminating in the Zagros orogenic event. The Zagros Orogeny, which was most active in the late Miocene and Pliocene, resulted in closure of the Neo-Tethys Ocean and development of a foredeep (Hooper et al., 1995), reactivation of older fault systems, and the compressional folding and faulting that characterize the present Zagros fold belt (Beydoun, 1988; Ameen, 1991, 1992; Hessami et al., 2001). Final uplift in the Holocene was accompanied by erosion that was locally extensive in the fold belt. The structural evolution of the Mesopotamian Basin and Zagros fold belt is reflected in the orientation of the present structures in these regions. The Mesopotamian Basin, which was relatively unaffected by tectonic compression, is mildly folded with increasing deformation eastward approaching the Zagros Mountains (Figure 1). Broad, pre-Neogene folds are oriented N-S in the southern part of the basin. The structurally complex Zagros fold belt is characterized by a linear, NW-SE fold and fault pattern that was imposed during late Paleogene and Neogene tectonism. Narrow, en-echeleon compression structures, locally continuous for more than 100 km, developed during this event. The present seismicity indicates that the Mesopotamian Basin and Zagros fold belt are still tectonically active (Jackson and McKenzie, 1984; Hessami et al., 2001).

The Mesozoic-Cenozoic stratigraphic section and lithostratigraphic units (formations and groups) that define the regional 3-D model are illustrated in Figure 2. The stratigraphic section varies from a maximum thickness of about 6.5 km along the axis of the Mesopotamian Basin to thicknesses of 3–5 km at the basin's western margin. In the Zagros fold belt, the temporally-equivalent section ranges in thickness from approximately 3 km in topographic lows to less than 1.5 km on topographic highs.

During the late Mesozoic and early Cenozoic, sedimentation in the area of the present Mesopotamian Basin and Zagros fold belt was controlled by local tectonics, eustatic sea-level changes, and climate variations. From Jurassic through Late Cretaceous time, sea-level fluctuations in conjunction with slow subsidence led to the formation of large, but shallow intrashelf basins on the passive margin of the Neo-Tethys Ocean and the Arabian Plate (Stoneley, 1987; Alsharhan and Nairn, 1997; Murris, 1980). Organic-rich sediments, which gave rise to the (Jurassic) Sargelu and Naokelekan source rocks (Figure 2), accumulated in these basins under anoxic conditions, and high-energy carbonates (i.e., bioclastic and oolitic) were deposited along the basin margins on the carbonate-evaporite shelf. In the Late Jurassic, depositional conditions culminated in the formation of thick evaporites (anhydrite and salt), which presently form a semi-permeable regional seal (i.e. Gotnia Formation) above the Jurassic source facies (Figure 2). The distribution of Cretaceous reservoirs in the southern Mesopotamian Basin was influenced by the nature of these evaporites (Murris, 1980; Beydoun et al., 1992).

Marine carbonate sedimentation predominated throughout most of the Cretaceous and Tertiary; however, the sedimentary record documents numerous unconformities and periods of nondeposition during that time. In the early to middle Cretaceous, a large influx of clastic sediment from the Zubair and Burgan deltas to the west and southwest prograded across the inner carbonate-shelf area (Alsharhan and Nairn, 1997), and deposited the sandstones of the Zubair and Burgan Formations (Figure 2). The Zubair Formation is the main reservoir unit in giant and supergiant fields in the southern Mesopotamian Basin. The Cretaceous section shows a decrease in clastic material and an increase in

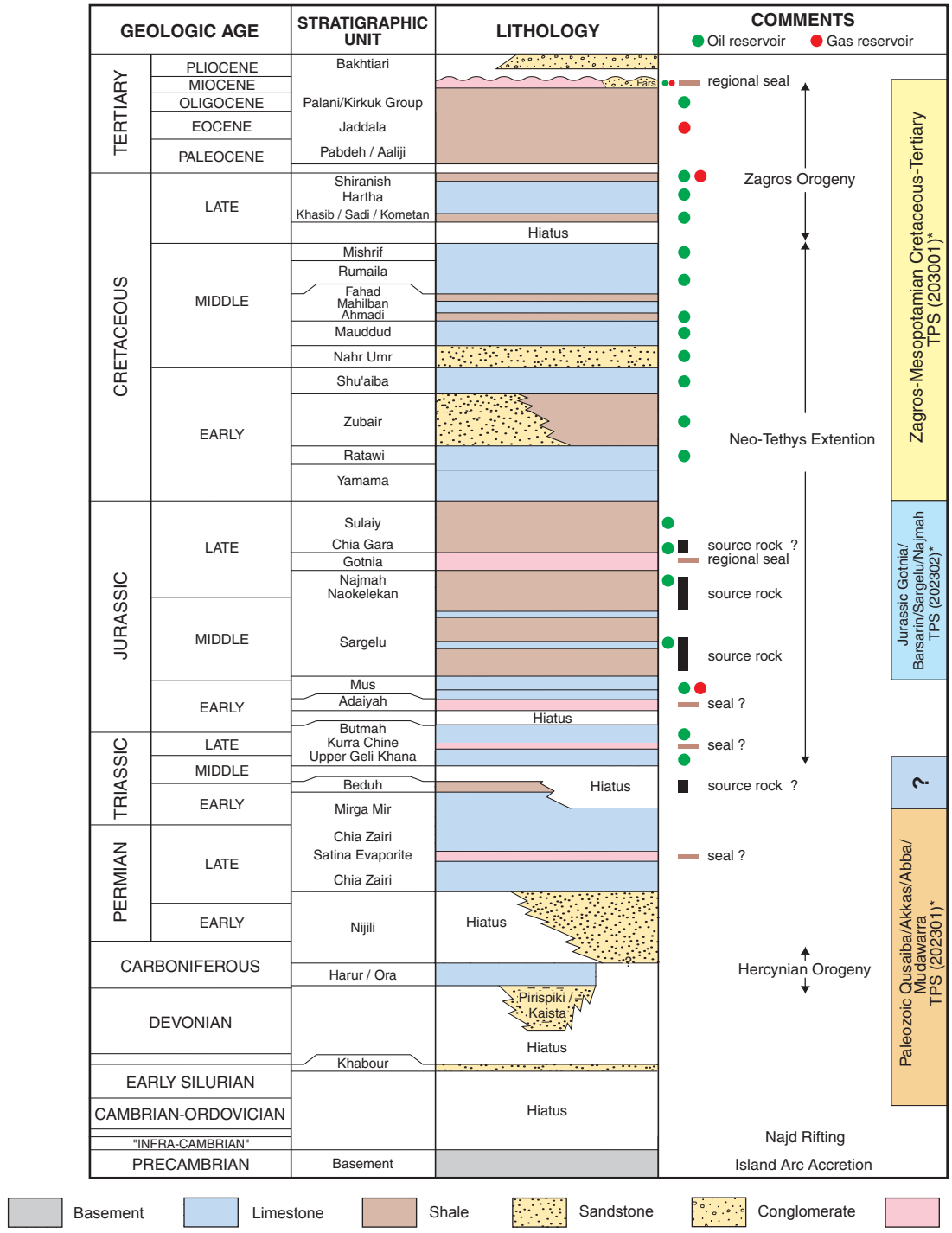

Figure 2: Stratigraphic section and major tectonostratigraphic phases relevant to the Paleozoic, Jurassic, and Cretaceous-Tertiary Total Petroleum Systems (TPS) of Iraq (modified from Verma et al., 2004). Stratigraphic names include equivalent names for chronostratigraphic units incorporated in the model (see Table 1). Total Petroleum Systems and their six digit numeric codes are shown in comments column. The portion of the Jurassic TPS and Cretaceous-Tertiary TPS in Iraq (see inset map on Figure 1) formed the basis of the regional petroleum-system model.

pelagic limestone in the late Cenomanian (Sadooni and Aqrawi, 2000). From the Late Cretaceous through the middle Miocene, intrashelf basins consolidated to form a single NW-trending basin that progressively was infilled with marine carbonates and shales. Infra-Cambrian salt tectonics influenced sedimentation in the south throughout this period (Beydoun et al., 1992). Deposition during the late Eocene to early Miocene was dominated by formation of shallow-marine limestones and dolomites. Reef limestones deposited along the basin shelf form the reservoir rocks of the Oligocene Kirkuk Group

(Figure 2), the main oil pay in the Kirkuk structure. In the middle Miocene, evaporites accumulated in numerous restricted sub-basins that formed as tectonic compression increased. In the late Miocene and Pliocene, during the main Zagros tectonic event, a thick wedge of fine-to-coarse-grained sandstone and conglomerate, shed from the rising Zagros Mountains, was deposited in the rapidly subsiding Zagros foredeep (Beydoun et al., 1992; Sadooni and Aqrawi, 2000). Deposition of these clastics represents the transition from marine to continental conditions and the final filling of the foredeep basin.

TOTAL PETROLEUM SYSTEM

The essential geologic elements required for petroleum accumulation in the Mesopotamian Basin and Zagros fold belt include Jurassic source rocks, Cretaceous and Tertiary reservoirs and seals, and Paleozoic and Paleogene/Neogene structural traps (Alsharhan and Nairn, 1997). These elements and the total petroleum-system processes (generation, migration, accumulation) that took place in the basin and fold belt are discussed in the following sections as they relate to the model simulations.

Source Rocks

The Middle Jurassic Sargelu Formation and the Upper Jurassic Naokelekan Formation (Figure 2) yielded the bulk of the oil that charged reservoir rocks in the Mesopotamian Basin and Zagros fold belt (Beydoun et al., 1992; Sadooni, 1997; Al Shididi et al., 1995). Organic-rich rocks of Cretaceous age also have been cited as sources of oil (Al Habba and Abdullah, 1989; Stoneley, 1990; Beydoun et. al., 1992; Beydoun, 1991, 1993; Al Shididi et al., 1995; Alsharhan and Nairn, 1997); however, compared to Jurassic source facies, these rocks overall, contributed only small amounts of oil to the total petroleum system, thus they were not considered in the model.

The thickness of the Sargelu Formation ranges from 100–400 m in the southern Mesopotamian Basin and from 100–200 m along the Zagros foredeep and in the northern part of the fold belt (Figure 3). Lithologically, the Sargelu is fairly uniform across the region (see Figure 3), and consists of argillaceous and bituminous limestone and calcareous shale. The lower 40 m of the section commonly has high source potential (PGA, 2000). The Naokelekan Formation is a condensed section ranging from approximately 5–45 m thick (Sadooni, 1997; PGA, 2000). The formation is composed of bituminous dolomite and limestone and bituminous shale that grade upward into fossiliferous, dolomitic limestone, bituminous shale, and limestone (Buday, 1980). Source-rock facies in the Sargelu and Naokelekan Formations grade westward into non-source rocks. In western Iraq outside the model area, Middle and Upper Jurassic strata have been eroded, and Lower Jurassic rocks consisting of interbedded sandstone, shale, and limestone with abundant chert (Bellen et al., 1959) and no known source potential, crop out over the Rutbah-Ga'ara uplift (see Figure 1).

Total organic carbon (TOC) content and initial hydrogen index (HI) were defined for the source-rock facies in the 3-D model. Overall, measured TOC values of potential source rocks are sparse and few data are available. The TOC contents of most shales in cores and cuttings from the Sargelu Formation in the fold belt (data have not been reported for the Mesopotamian Basin) range from 2% to more than 6%, with some values exceeding 20% in the lower part of the section (Al Habba and Abdulla, 1989; PGA, 2000). In contrast, surface samples of the Sargelu Formation where it is exposed (thrust zone; see Figure 1) commonly have TOC values of 2% or less (Al Habba and Abdulla, 1989; PGA, 2000). Shales in the Naokelekan Formation in the subsurface of the fold belt have TOC contents comparable to those of the Sargelu Formation, from 3–9%, and locally TOC values are higher than 15% (Al Habba and Abdulla, 1989; PGA, 2000). In outcrops in the thrust zone, the TOC contents of shales in the Naokelekan are variable, ranging from 0–11% (Al Habba and Abdulla, 1989; PGA, 2000). For the purposes of the model, 5% was adopted as an average TOC value for both formations.

The initial HI potential of the Sargelu and Naokelekan Formations was defined as 600 mgHC/g TOC based on the average composition of kerogen in the source rocks. The present HI values in these formations range from less than 100 to more than 600 mgHC/g TOC (Al Habba and Abdulla, 1989; PGA, 2000). Two samples of source rock from the Naokelekan, one each from Kirkuk and Taq Taq fields, have low HI values and high T_{max} values that are indicative of oil-generation completion at relatively shallow burial depths. The sample from Kirkuk field (Kirkuk 109 well; see Figure 1) has an HI value of 69 mgHC/g TOC and a T_{max} of 450°C at a depth of 3,396 m (PGA, 2000) and the sample from Taq Taq field (Taq Taq 1 well) has an HI value of 22 mg/g TOC and a T_{max} of 568°C at a depth of 3,236 m (Sadooni and Alsharhan, 2003).

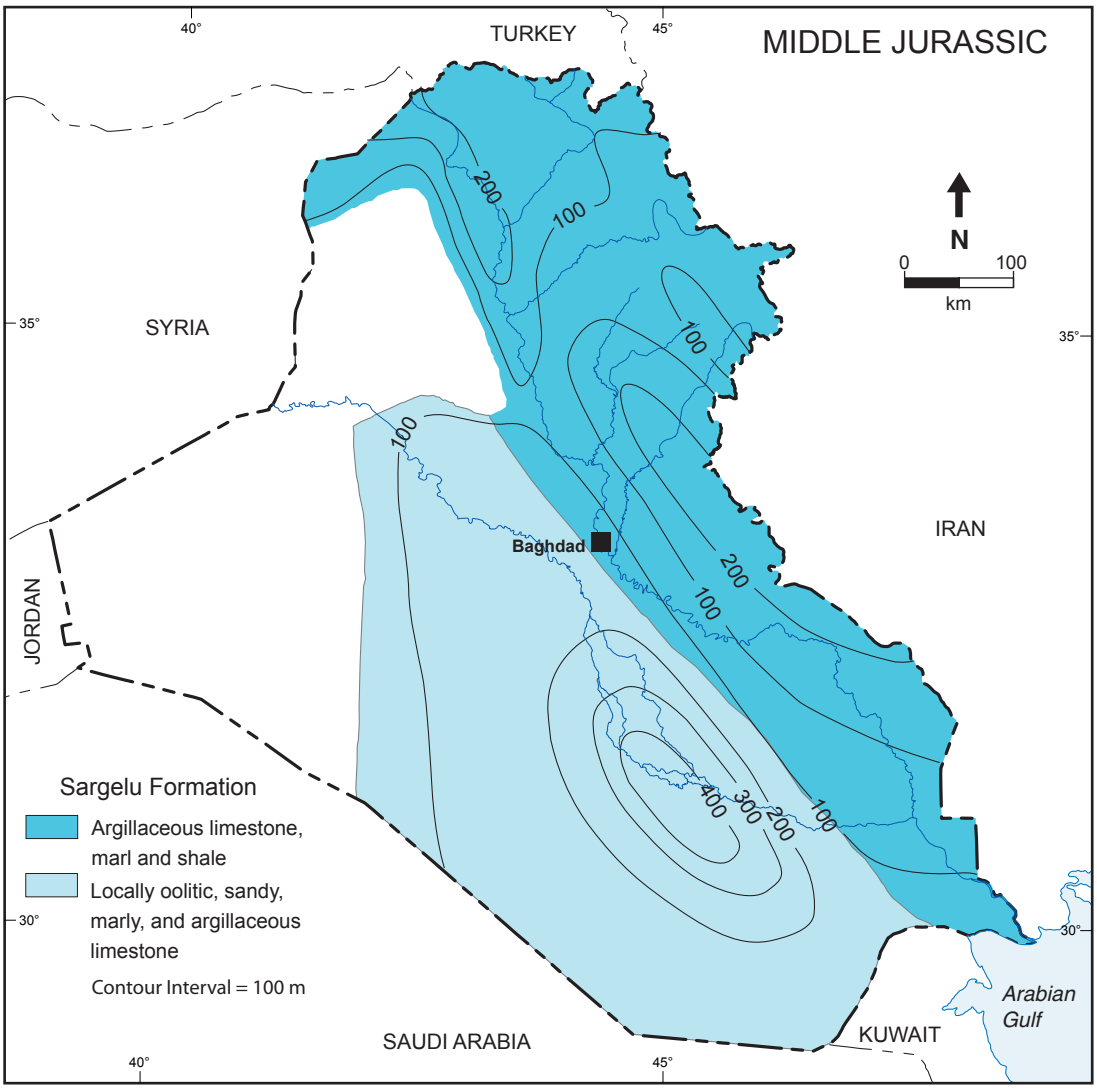

Figure 3: Map showing isopach contours and lithofacies for the Sargelu Formation (modified from GeoDesign, written communication, 1999).

Reservoirs and Seals

Cretaceous and Tertiary rocks are the principal reservoirs containing oil derived from Jurassic source rocks. Cretaceous reservoirs account for 76% of the petroleum resources in the southern part of the Mesopotamian Basin (Al Gailani, 2003), and most of these reservoirs are at depths greater than 3 km. The remaining petroleum production (23.9%) is from Tertiary reservoirs in the Zagros fold belt at burial depths less than 2 km, with minor production (0.1%) from Jurassic, Triassic, and Ordovician reservoirs (Al Gailani, 2003). Free gas has been encountered locally in Tertiary reservoirs along the eastern margin of the fold belt; however, the Mesopotasmian Basin and Zagros fold belt are dominantly oil-prone regions.

The main oil reservoirs in the Cretaceous and Tertiary stratigraphic section are carbonates (Beydoun et al., 1992); however, major sandstone reservoirs of Cretaceous age are present but less common in the southern Mesopotamian Basin. The porosity and permeability of carbonate rocks vary greatly depending on the unit, and can exceed 30% and 1,000 mD (Beydoun et al., 1992). Locally, the porosity in carbonates was enhanced by karstification and fold-related fracturing (Beydoun et al., 1992). The principal oil-bearing sandstones experienced diagenetic alteration (Al Shdidi et al., 1995; Sadooni and Aqrawi, 2000; Sadooni and Alsharhan, 2003); however, the nature and extent of these alterations and their effect on sandstone reservoir quality have not been well documented. Porosity in reservoir sandstones ranges from 1–30% and permeability varies from 0.1 to more than 5,000 mD (IHS Energy Group–formerly PetroConsultants, 1996).

Cretaceous shales are the top seals for many large oil reservoirs in the Mesopotamian Basin (Alsharhan and Nairn, 1997). Upper Jurassic anhydrite (Gotnia Formation), superjacent to Jurassic source facies, is a regional seal; although in many areas its sealing capacity is ineffective due to facies changes and/or basement-induced fracturing (Beydoun et al., 1992; Sharland et al., 2001). In the fold belt, Miocene-age supratidal evaporites and sub-unconformity pinchouts initially sealed petroleum traps, but many of the seals have been breached by fracturing and erosion (Beydoun et al., 1992).

Traps

Petroleum exploration in the Mesopotamian Basin and Zagros fold belt has focused predominantly on structural traps and secondarily on stratigraphic traps. In the southern Mesopotamian Basin, the principal trapping structures are large, broad, NS-striking, basement-cored anticlines that began forming in the Paleozoic, with continued but more limited growth throughout the Mesozoic and early Cenozoic (Ibrahim, 1983; Beydoun et al., 1992). Trap-forming mechanisms can be linked to reactivation of deep-seated Precambrian faults and diapiric growth of infra-Cambrian (Hormuz and equivalent) salt. Synorogenic faulting in the Mesozoic, with more restricted movement in the Cenozoic, triggered the growth of infra-Cambrian salt structures, which caused large drape folds to develop over basement fault blocks. Petroleum trapping is mostly within fault-block anticlines overlying evaporites.

In contrast to the broad structures in the southern Mesopotamian Basin, traps in the fold belt are dominated by NW-trending compressional folds that formed by inversion over extensional faults (Ameen, 1992; Hessami et al., 2001). Some structures are continuous for tens to hundreds of kilometers, with more than a thousand meters of throw. Trap development in the present-day fold belt and adjacent areas involved multiple phases of folding (Sharland et al., 2001). The initial stage occurred in the Mesozoic (Late Cretaceous) and is manifested in the thrusted and imbricated zones east of the fold belt. If the Mesozoic tectonic phase affected the area of the fold belt, it was subsequently overprinted by late Cenozoic folding and faulting. The major period of structural deformation and trap formation in the fold belt took place during the late Paleogene and Neogene, Zagros orogenic event.

BASIN MODELING

A regional 3-D total petroleum-system model was developed to simulate burial-thermal history, source-rock maturity, and petroleum generation and migration in the Mesopotamian Basin and Zagros fold belt. The model is a numerical formulation of the region's history based on interpretation of combined geologic, geophysical, and geochemical data in a temporal framework, and it includes the principal elements (source rocks, reservoir rocks, and seals) of the total petroleum system. Vertical data (1-D profiles) were extracted from the 3-D model at three key oil fields to evaluate burial-thermal history, and timing and extent of petroleum generation (see Figure 1 for locations): (1) Zubair field in the southern Mesopotamian Basin, (2) Khashim Ahmar field in the southern fold belt, and (3) Kirkuk field (at Baba dome) in the northern fold belt. Zubair and Kirkuk fields were selected because they are major accumulations with more comprehensive vitrinite reflectance (R_o) and geochemical data (PGA, 2000) than other fields in their respective regions. Khashim Ahmar field is of interest because it is situated in a paleo-depocenter in the present-day fold belt, although no source rock or thermal maturity data are available for the field.

In the regional 3-D model, thermal maturity and petroleum generation and expulsion histories were simulated on a cell-by-cell basis, and model results were extracted for the top Middle Jurassic surface at ages (25 Ma, late Oligocene; 10 Ma, middle Miocene; 8 Ma, late Miocene; and present day) that corresponded to periods of major petroleum generation and expulsion. It is important to note that 3-D modeling with fully integrated pressure, volume, and temperature (PVT) calculations between neighboring cells was not feasible for the regional area of interest due to the long processing time required to compute the model.

Secondary migration and accumulation of petroleum were simulated for the periods specified above using a combination of PVT-controlled 3-D modeling and flow-path modeling. Full 3-D modeling best describes petroleum migration processes (i.e. vertical versus lateral flow) because it takes into account bouyancy, and pore-fluid and capillary pressures and correctly handles the physical (carrier-seal) relations within the total petroleum system. However, full 3-D modeling results in long processing times; thus, it was restricted to small areas of interest within the regional model. Flow-path calculations

were performed on chronostratigraphic structure surfaces computed by the regional 3-D model without reference to the complete set of surfaces that define the model. Flow-path modeling is based on the premise that migration occurs instantaneously by buoyancy and that flow is focused near the top of a carrier unit; however, it does not consider the physical interactions that take place during migration. The advantage of flow-path modeling is that potential migration pathways can be geometrically computed for a large (basin-scale) area of interest within a short period of time, but the disadvantage is that it is based on simplistic assumptions of migration systems.

Model Development

Chronostratigraphic Units

A detailed subsurface structure map drawn on the top Middle Jurassic surface (Christian, 1997) and thirteen generalized, chronostratigraphic isopach-lithofacies maps of the Mesozoic-Cenozoic section (written communication, GeoDesign, 1999) provided geologic control for the regional 3-D model (Table 1). The contour data on the maps were digitized and interpolated into grids with a cell dimension of 1,000 m. The 3-D model was constructed by stacking the chronostratigraphic succession of unit-thickness grids on the top Middle Jurassic surface grid. The base of the Middle Jurassic unit served as the bottom of the model, and digital-surface elevations defined the top. The resulting 3-D block consists of 14 chronostratigraphic units and 512 by 1,220 cells.

Chronostratigraphic units in the model were assigned absolute ages of deposition, and amounts and ages of erosion and/or periods of nondeposition were defined. The ages of depositional and erosional events were designated based on the geologic time scale of Haq et al. (1987); however, temporal correlation between depositional sequences in the basin and sequences on the Global Cycle Chart is imprecise. Lithologies, represented as end-member rock types or as compositional mixtures were assigned to the facies in each unit. The physical and thermal properties of the rock types and mixtures, including their thermal conductivities and heat capacities were either user-defined or software default values.

Inevitably, assumptions are intrinsic to the model due to the generalized nature of the map information, and because of a general lack of adequate calibration data. Limitations also arise from the need to simplify complex geologic relations within the large area that encompasses the petroleum system. One example is the structural complexity of the Zagros fold belt, which could not be accurately reconstructed with the available data. Despite these limitations, the 3-D model, as designed, is a generalized representation of the geologic history that can be used to evaluate the total petroleum system on a regional scale.

Temperature and Heat Flow

Determining the timing of petroleum generation and expulsion required calibration of the thermal regime in the regional 3-D model. Parameters used in the calibration included heat flow, thermal conductivity of the rock matrix, surface temperature, and sediment thickness (present and past). Of these factors, heat flow is the least constrained parameter. Reservoir and bottom-hole temperature data for six wells (Ibrahim, 1983; 1984; IHS Energy Group, 1996) were used to estimate the present heat flow in the Mesopotamian Basin and Zagros fold belt (Figure 4). A good fit between calculated and measured temperature values was achieved using estimated heat-flow values that varied from 45 mW/m^2 in the southern Mesopotamian Basin to 48 mW/m^2 in the fold belt, assuming a mean surface temperature of 27°C throughout the region. It is noteworthy that average continental heat flow (~65 mW/m^2) did not produce matching temperatures. Based on the parameters defined in the thermal model, computed geothermal gradients for the wells in the Mesopotamian Basin vary locally from 17 to 20°C/Km, and are in agreement with published temperature gradients for this region (Ibrahim, 1983; 1984). In the Zagros fold belt, calculated thermal gradients are similar to those in the south, varying from 18 to 23°C/Km.

Vitrinite reflectance (% R_o), which integrates the effects of temperature over time, was used to evaluate the paleothermal history of the Mesopotamian Basin and Zagros fold belt. Measured R_o values for six widely-spaced wells (PGA., 2000) provided the input for the analysis. Calibration of the paleothermal regime required matching measured R_o values for each well with values of R_o calculated using the EasyR_o method of Sweeney and Burnham (1990). A reasonable correlation between measured and

Table 1

Interval	Unit	Stratigraphic Unit	Deposition (Ma)	Erosion (Ma)
			From – To	From – To
*Upper Miocene to Recent	O	Dibdiba, Upper Fars, Bakhtiari Formations	10.2 – 5.2	5.2 – 0
Middle Miocene	N	Lower Fars Formation	16.2 – 10.2	
Lower Miocene	M	Jeribe, Euphrates, Dhiban, Ghar, Serikagni Formations	25.2 – 16.2	
Oligocene	L	Bajwan, Baba, Anah, Azkand, Shurau, Sheikh Alas, Tarjil, Palani, Ibrahim Formations, Kirkuk Group	36.0 – 25.2	
Middle Eocene to Upper Eocene	K	Dammam, Gercus, Pila Spi, Avanah, Jaddala Formations	49.0 – 36.0	
Paleocene to Lower Eocene	J	Rus, Umm-er-Radhuma, Sinjar, Kolosh, Aaliji, Khurmala Formations	66.5 – 49.0	
Upper Cretaceous (Upper Campanian to Maastrichtian)	I	Tayarat, Hartha, Safawi, Aqra, Bekhma, Shiranish, Tanjero Formations	84.0 – 68.0	68.0 – 66.5
Upper Cretaceous (Turonian to Lower Campanian)	H	Sad`I, Mushurah, Wajnah, Tanuma, Khasib, Kometan Formations	92.0 – 84.0	
Upper Cretaceous (Cenomanian)	G	Rutbah, M`Sad, Gir Bir, Mishrif, Rumaila, Kifl, Ahmadi, Dokan, Balambo Formations	96.0 – 92.0	
Upper Cretaceous (Upper Albian)	F	Mauddud, Jawan, Qamchuqa, Balambo Formations	108.0 – 96.0	
Lower Cretaceous (Valanginian to Aptian)	E	Shu`aiba, Yamama, Zubair, Ratawi, Balambo, Sarmord, Garagu, Qamchuqa Formations	131.0 – 108.0	
Upper Jurassic (Callovian to Kimmeridgian)	D	Najmah, Gotnia, Barsarin	151.0 – 131.0	
Upper Jurassic (Callovian to Kimmeridgian)	Naokelekan	Naokelekan Formations – Source Rock	157.0 – 151.0	
Middle Jurassic (Callovian)	Sargelu	Sargelu Formation – Source Rock	169.0 – 163.0	163.0 – 157.0
Middle Jurassic (Callovian)	C	Muhawir Formation	179.0 – 169.0	

Chronostratigraphic units and ages of depositional and erosional events used in the development of the regional 3-D model. Stratigraphy (formations and groups) from GeoDesign, 1996. Event ages from Haq, 1987. Asterisk (*); designation of original unit (upper Miocene-Pliocene) modified to include recent sediments.

modeled values was achieved by adjusting the estimated amount of stratigraphic section eroded at each well location (see following discussion) and by varying the regional heat-flow. Ultimately, the paleoheat flow that provided the best calibration of the data was 60 mW/m^2 for the Middle and Late Jurassic followed by a linear decay to the estimated present-day values (45 mW/m^2 in the Meopotamian Basin and 48 mW/m^2 in the fold belt). Steady-state heat-flow conditions (i.e., surface heat-flow equals the heat flow at the base of the sedimentary section) were assumed at all times.

Timing and Amount of Erosion

Modeled R_o-depth trends constructed for the paleothermal analysis were used to estimate the amount of Cenozoic strata eroded in the model area. In each of six wells, the R_o trend that best fit the data was extrapolated to an R_o value of 0.25%, which was assumed to approximate the vitrinite refelctance at surface conditions (Figure 5). Computed R_o trends for three wells (one in the central Mesopotamian Basin and the others in the southern part of the basin) intersect the present-day surface at approximately 0.25–0.30% R_o, indicating that erosion during late Cenozoic time generally was minimal (less than 500 m) in this region. In contrast, calculated R_o trends for three wells in the central Zagros fold belt when extrapolated to a value of 0.25% indicate that approximately 1,500 m of Cenozoic (late Tertiary-Quaternary) section was exhumed by erosion. Near the thrust belt to the northeast, maximum erosional loss may have been as high as 2,000 m, as indicated by estimates of eroded Tertiary section in the Dezful embayment area of Iran along strike to the southeast (Bordenave and Burwood, 1990). Prior to the extensive loss of stratigraphic section during the late Cenozoic, episodic erosion also occurred locally in the late Mesozoic (i.e. K/T boundary, Cenomanian-Turonian, Berriasian-Aptian events), which resulted in exhumation and reworking of Middle Jurassic to Upper Cretaceous sediments in uplifted areas close to the Zagros Mountains (Dunnington, 1958). The amount of stratigraphic section removed during Mesozoic erosional episodes has not been reported; however, sensitivity tests indicate that pre-Tertiary erosion, although locally intense, had little impact on the Jurassic source-rock maturation history.

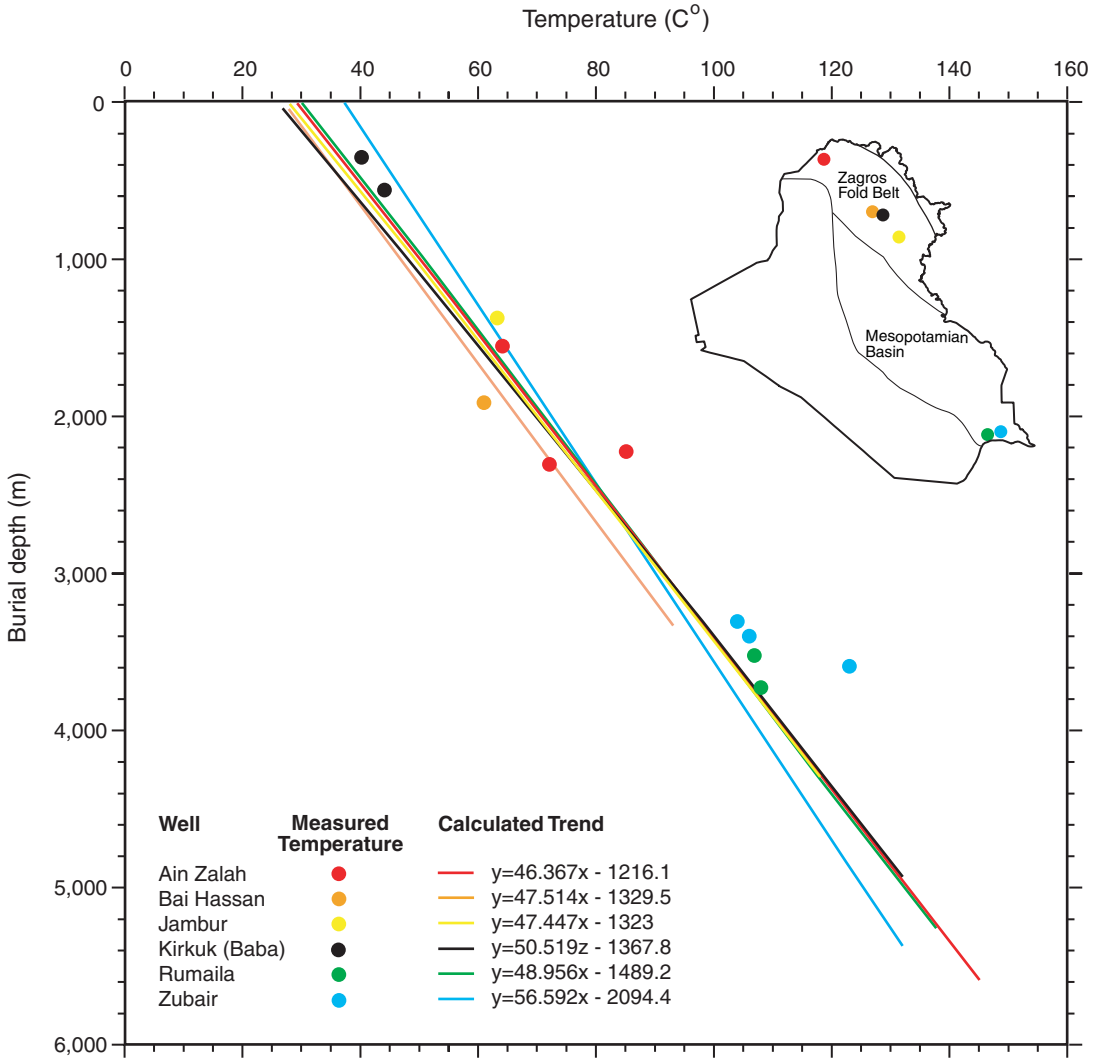

Figure 4: Modeled thermal gradients and measured temperature values used in calibrating the regional 3-D model. See inset map for well locations. Temperature data are from IHS Energy Group (1996) and include individual reservoirs and corrected bottom-hole temperature measurements.

Erosion was simulated in the regional 3-D model by populating the finite-element grid with values corresponding to the amount of eroded Cenozoic section computed at each grid point. Values varied from zero (no erosion) in the Mesopotamian Basin to 2,000 m (maximum erosion) in the northeastern part of the fold belt. In areas of the model with no data, amounts of erosion were interpolated from these end-member values. The cumulative eroded Mesozoic section was assumed to be minimal (~50 m) and was not included in the model.

Reservoir Pressures

Fluid pressures calculated in the regional 3-D model were evaluated for an area of interest in the southern Mesopotamian Basin where PVT-controlled 3-D modeling was performed. The regional model simulated pore-fluid pressures using the permeabilities of the lithologies defined for the model units. Permeability data were not available to calibrate the model; however, fluid-pressure measurements from mud weights and drill-stem tests reported for a few wells (Ibrahim, 1983; IHS Energy Group, 1996) constrained the calculated pressures. Compilation of pressure data revealed that reservoir pressures are slightly higher than hydrostatic pressures at depths less than 3,700 m, but increase rapidly to values (50–60 Mpa) approaching lithostatic pressures at depths greater than 3,700 m. A comparison of calculated pressures and the measured pressure values relative to this depth generally showed good agreement, which indicated that the software default permeabilities used in the model were reasonable.

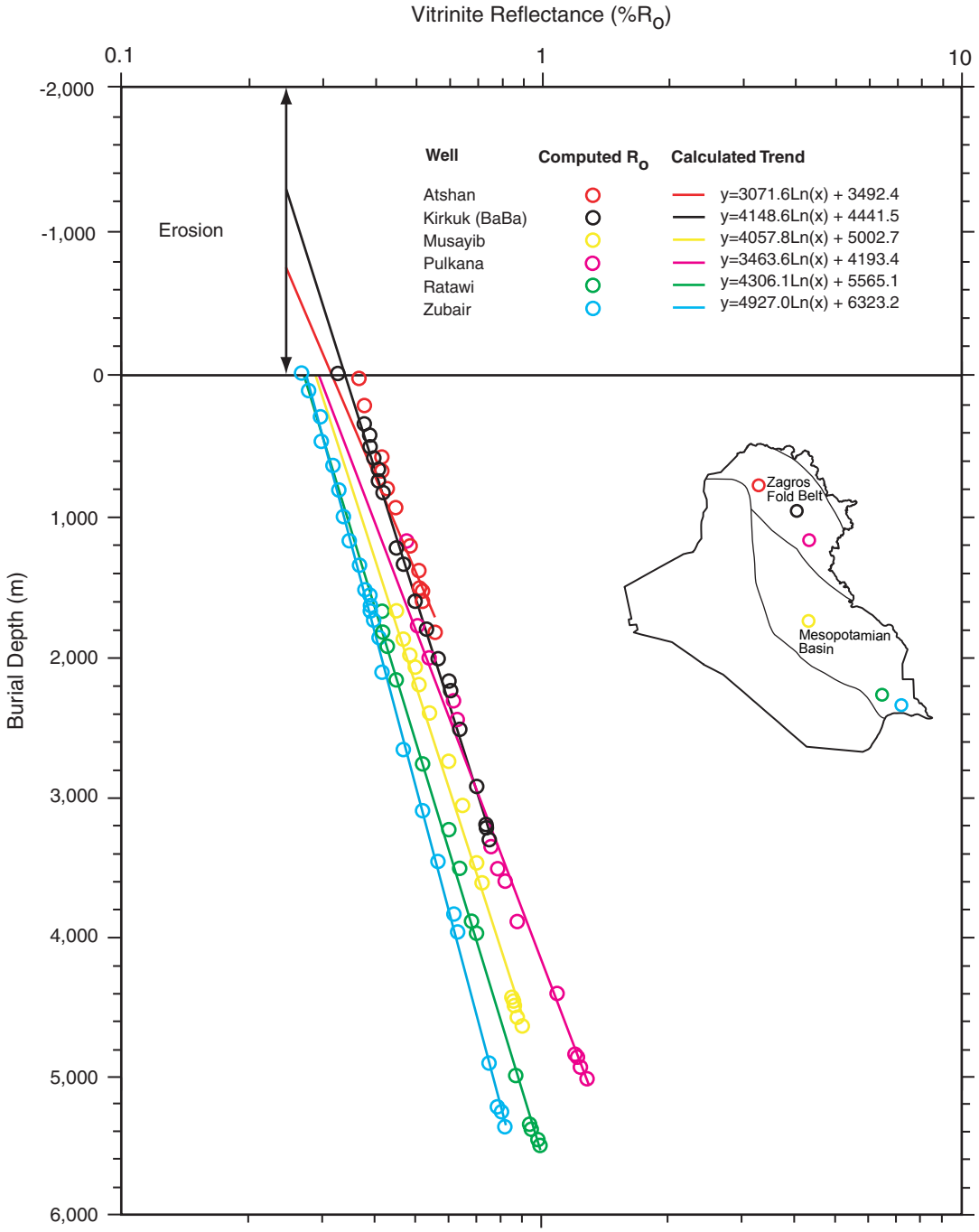

Figure 5: Calculated R_o values and modeled vitrinite reflectance (R_o) trends for wells in the study area. See inset map for well locations. Modeled trends were computed based on values of R_o calculated by the EasyR$_o$ method (Sweeney and Burnham, 1990). Extrapolation of trends (shown as dashed lines) provided estimates of Late Tertiary and Quaternary erosion.

Petroleum Generation Kinetics

The relation between the atomic S_{org}/C ratio in Type-IIS kerogen, and the level of thermal maturity at which oil generation occurs in Type-IIS kerogen-rich source rocks, is reflected in the kinetic parameters used in the regional 3-D model. Samples of Jurassic carbonate source rock were not available to determine the organic sulfur contents of the kerogen in the organic matter; however, based on the method of Hunt et al. (1991), the sulfur content of the oils from these sources provides a first approximation. The sulfur-API gravity relation, as proposed by Orr (2001), indicates that oils derived from Jurassic carbonate facies in Iraq were generated from Type-IIS kerogen. This kerogen type typically has a moderate to high organic-sulfur content with atomic S_{org}/C ratios greater than 0.04 (Orr, 1986).

Laboratory pyrolysis and maturation studies of subsurface samples have demonstrated that moderate to high organic-sulfur contents in kerogen (atomic $S_{org}/C > 0.04$) result in oil generation at low thermal maturities (Tomic et al., 1995; Lewan, 1985; 1998; Tannenbaum and Aizenshtadt, 1985; Orr, 1986; Petersen and Hickey, 1987; Baskin and Peters, 1992). Examination of kinetic parameters indicates that open-system (Rock-Eval) pyrolysis greatly underestimates the timing and extent of oil generation of Type IIS kerogen compared to isothermal hydrous pyrolysis because sulfur, which initiates the oil-generation reaction, has a short residence time under open-system conditions (Lewan, 1998; Lewan and Ruble, 2002). The kinetic parameters determined by open-system pyrolysis are based on a composite product of bitumen, oil, and gas, which consists of approximately 60 wt. % non-hydrocarbons (i.e. nitrogen, sulfur, oxgen compounds; Behar et al., 1997). In contrast, isothermal kinetic parameters determined by hydrous pyrolysis are based on expelled oil that is similar in composition to natural crude oil.

The relationship between API gravity and the sulfur content of the produced oils in Iraq is similar to that of oils produced from the Permian Phosphoria Formation, USA. Based on the similarity in these oil compositions, isothermal kinetic parameters for Type-IIS kerogen in the Phosphoria (activation energy = 42.71 kcal/mol; frequency factor = 4.31×10^{23} m.y.$^{-1}$; Lewan and Ruble, 2002) were used as an analog for modeling oil generation in Jurassic source rocks. Using these kinetics as an analog assumes that the atomic mean S_{org}/C ratio for Type-IIS kerogen in Jurassic source rocks approximates the atomic S_{org}/C ratio for kerogen in the Phosphoria (0.045). Based on the isothermal kinetics defined for the Phosphoria, the regional 3-D model yields results that are consistent with geochemical data reported for Kirkuk oil field (Kirkuk 109 well) in the Zagros fold belt (Al Habba and Abdulla, 1989; PGA, 2000).

It is noteworthy that atomic S_{org}/C ratios for Type-IIS kerogen can be as high as 0.094 (Orr and Sinninghe Damste, 1990). If the atomic S_{org}/C ratios in Jurassic source rocks exceed 0.045 and are as high as 0.094 then the possibility exists that oil generation in the Mesopotamian Basin and Zagros fold belt occurred at an earlier time and at lower thermal maturities than the model predicts, and that the extent of generation is greater than currently modeled. It should be noted that Rock-Eval kinetics for Type II kerogen have been reported for Kirkuk field in northern Iraq (Tissot et al., 1987). However, the kerogen on which the determinations were based had low TOC values (~1 wt. %); moreover, the frequency factor was not cited, thus these kinetics were not used to model petroleum generation.

The hydrous-pyrolysis-kinetic parameters of Knauss et al. (1997) were used to evaluate the timing and extent of gas (methane) generation in Jurassic source rocks. The Gaussian distribution of activation energies for the kinetics reported by Knauss et al. (1997) has a mean of 45.4 kcal/mol and a standard deviation of 0.87 kcal/mole, with a frequency factor of 7.89×10^{23} m.y^{-1}. In oil-prone kerogen, gas-to-oil ratios typically are less than 1,000 scf/bbl during main-stage oil generation (Lewan and Henry, 2001), indicating only minor gas is generated from this kerogen type. However, at high thermal stress levels, gas-to-oil ratios greatly increase as a result of oil cracking to gas (Lewan and Henry, 2001). To assess the extent and timing of oil cracking to gas in Jurassic source rocks and adjacent reservoirs, kinetic parameters determined by hydrous pyrolysis and hydrothermal pyrolysis methods (activation energy = 76 kcal/mol and frequency factor = 3.42×10^{33}m.y.$^{-1}$ for cracking of C_{15+} saturates) (Tsuzuki et al., 1999) were assigned in the regional 3-D model. Hydrous pyrolysis experiments (Hesp and Rigby, 1973) and deep subsurface oil accumulations at high thermal maturities (Ro > 1.35%) (Price, 1997) demonstrate that water enhances the thermal stability of oil.

The regional 3-D model simulates the generation of petroleum as two distinct fluid fractions**:** (1) black oil, with a molar mass of 90.072 g/mol, is produced by the kerogen-to-oil reaction; and (2) dry gas, with a molar mass of 17.943 g/mol, is generated by the kerogen-to-gas and the oil-to-gas cracking reactions. The ratio of black oil to dry gas is controlled by the proportion of the HI allocated to each fluid, which was determined in accord with the isothermal pyrolysis (oil, gas, oil-to-gas cracking) kinetics used in the model (black oil = 522 mgHC/gTOC; dry gas = 78 mgHC/gTOC). Depending upon pressure and temperature conditions, these fluids in the subsurface may be in either a liquid or a vapor phase.

Fault Properties

A structure map drawn on the top Middle Jurassic surface (Christian, 1997) and a prospect map (written communication, GeoDesign, 1999) provided the fault control for the regional 3-D model. In the Zagros fold belt, high amplitude normal faults were defined as semi-sealing in the horizontal direction (defined as a -5 log mD shift relative to the matrix permeability) and semi-open in the vertical direction (defined as a +5 log mD shift relative to the matrix permeability)**.** These fault properties

permitted cross-formation flow in the model while allowing for the trapping of petroleum in a vertical succession of reservoirs. Mapped faults in the Mesopotamian Basin are scarce (Christian, 1997; written communication, GeoDesign, 1999) but where present, they are associated with deep-seated features that typically have no surface expression, thus they were not included in the 3-D model. It should be noted that only major fault zones in the Zagros fold belt were incorporated in the regional model. Minor faults, and faults smaller than the model cell-size (1,000 m) were excluded to avoid an excessive number of model grid points.

Although Petromod software is a program that models petroleum generation and migration in sedimentary basins, it does not account for the effects of tectonic compression or hydrodynamic fluid-flow. The amount of fault throw and the fault dip also cannot be included in the model input, thus model simulations do not directly take into account the influence that crustal shortening and thickening may have had on petroleum migration.

MODEL ANALYSIS

Burial-Thermal History

The modeled burial history of Jurassic source rocks in the Mesopotamian Basin and Zagros fold belt is illustrated by the paleostructure on the top Middle Jurassic surface (Figures 6a–6d). Reconstructed depth-surfaces, as shown in Figures 6a-6d, are the products of sediment backstripping and decompaction through time, based on software default-compaction curves. Although the burial model is generalized, it reflects the gross geologic features of the basin and is consistent with the current understanding of the basin's geologic and tectonic history (Ameen, 1992; Beydoun et al., 1992; Sharland et al., 2001). Results of the model show that through middle Miocene time sedimentation was confined to two intrashelf basins that were affected by subtle structure, as indicated by the paleohigh between the intrabasin thick areas (Figures 6a and 6b). Beginning in the late Miocene, these basins coalesced as local platform deposition ceased and gave way to widespread sedimentation in the subsiding foredeep adjacent to the Zagros Orogen (Figure 6c). Sediment deposition continued in the foredeep from the late Miocene through the Pliocene (Figures 6c and 6d), causing a progressive shift in the foredeep axis westward to its present position.

At present-day, Jurassic source rocks in the Mesopotamian Basin are at or near maximum burial depth due to the absence of major erosion during the Cenozoic. Close to the Zagros Mountain front, source rocks are buried at depths greater than 6 km, but near the west margin of the basin, equivalent rocks are much shallower at about 3.7 km (Figure 6d). In the Zagros fold belt, Jurassic source rocks were deeper in the past (by 1-2 km) than they are at present. In the late Miocene, compressional folding along with deposition of reworked sediments increased the burial depths of source rocks to their maximum levels, which was followed by widespread erosion in the Holocene. In structural highs, source rocks presently are at depths of about 2 km, in contrast to structural lows where they are buried as deep as 5 km (Figure 6d).

In tectonically active regions, uplift or subsidence may alter the heat flow and geothermal gradient. Heat flow in subsiding basins with rapid accumulation of fine-grained sediment commonly is retarded resulting in below-average geothermal gradients. Basins with high sedimentation and subsidence rates can have heat-flow values as low as 41 mW/m^2 (Burrus and Audebert, 1990). The heat flows that best fit the calculated geothermal gradients in the Mesopotamian Basin and Zagros fold belt (45–48 mW/m^2) are low in comparison to normal continental heat flow, which varies from about 41–82 mW/m^2. The global average is in the range of 60–65 mW/m^2 (Lee and Uyeda, 1965; Gretener, 1981). These below average values are consistent with the high sedimentation rate during the late Miocene and Pliocene and indicate that the thick section of undercompacted sediments deposited in the foredeep has not thermally re-equilibrated.

One-dimensional burial-thermal profiles (Figure 7) demonstrate the effects that rapid burial had on source-rock temperatures. In the Mesopotamian Basin, Jurassic source rocks are presently at maximum burial temperatures, in contrast to the fold belt where the present temperatures are cooler than they were in the past. At Zubair field in the south (Figure 1), maximum source-rock temperatures are approximately 140°C at a depth of about 5,350 m (Figure 7a). The present burial temperatures of source rocks in Khashim Ahmar field to the north also are about 140°C, which correspond to a depth of approximately 4,400 m, but temperatures were as high as 150°C in the late Miocene when the rocks

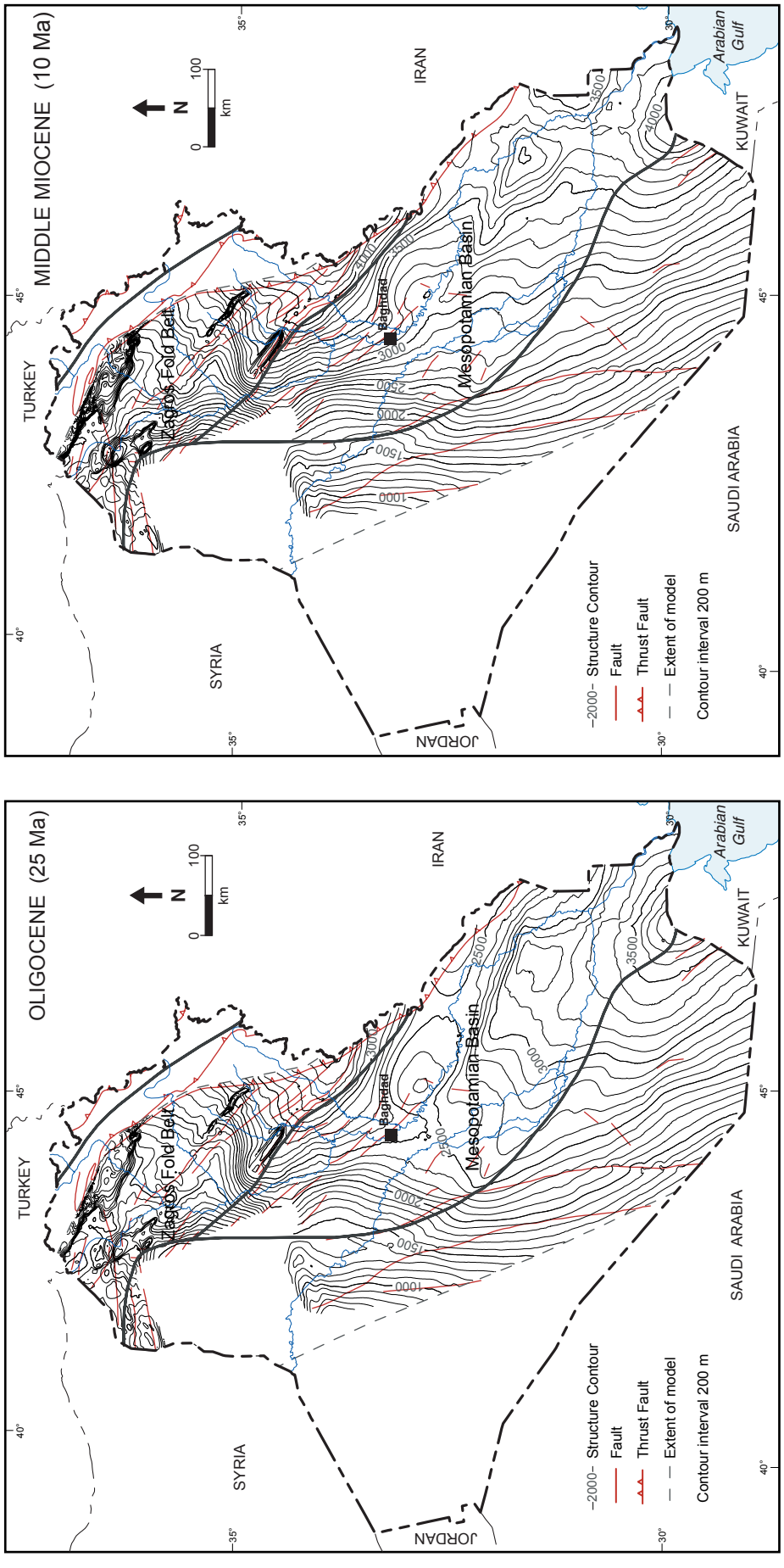

Figure 6: Modeled structure on the top Middle Jurassic surface at time periods:

(a) 25 Ma (late Oligocene), (b) 10 Ma (middle Miocene), (c) 8 Ma (late Miocene), (d) Present day. Present-day structure contours are from Christian (1997).

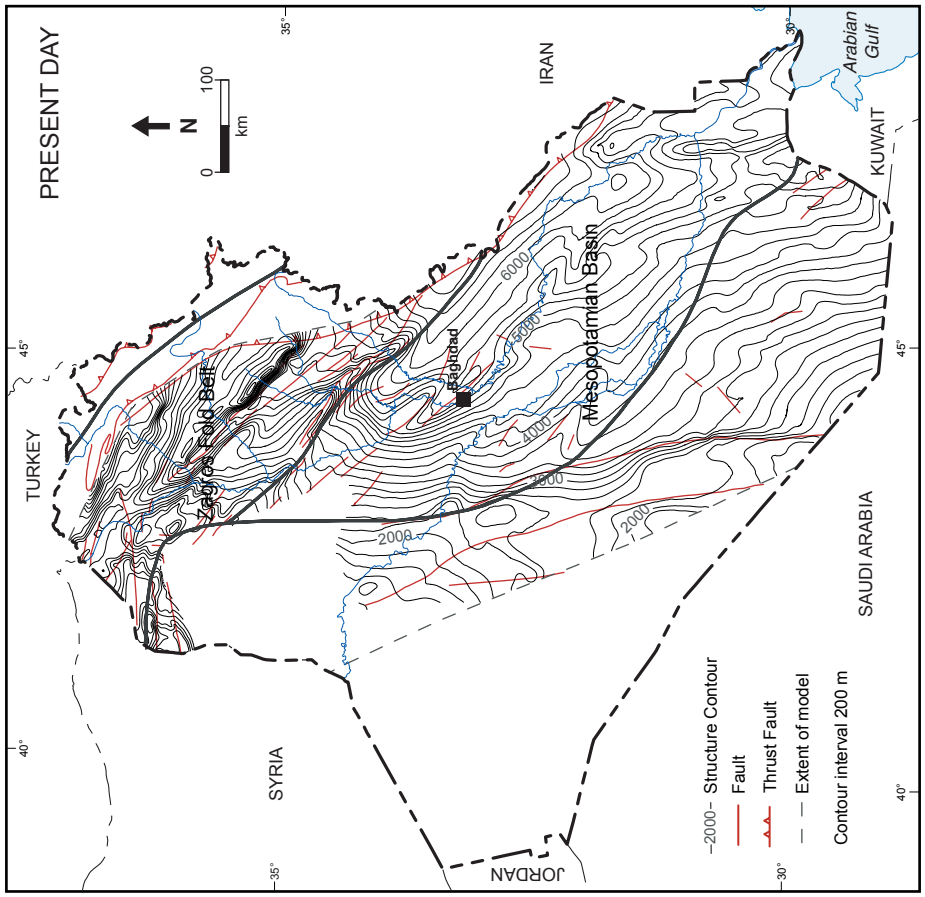
PRESENT DAY
TURKEY
SYRIA
IRAN
JORDAN
SAUDI ARABIA
KUWAIT
Arabian Gulf
Zagros Fold Belt
Mesopotamian Basin
Baghdad
N
0
100
km
2000
Structure Contour
Fault
Thrust Fault
Extent of model
Contour interval 200 m

(d)

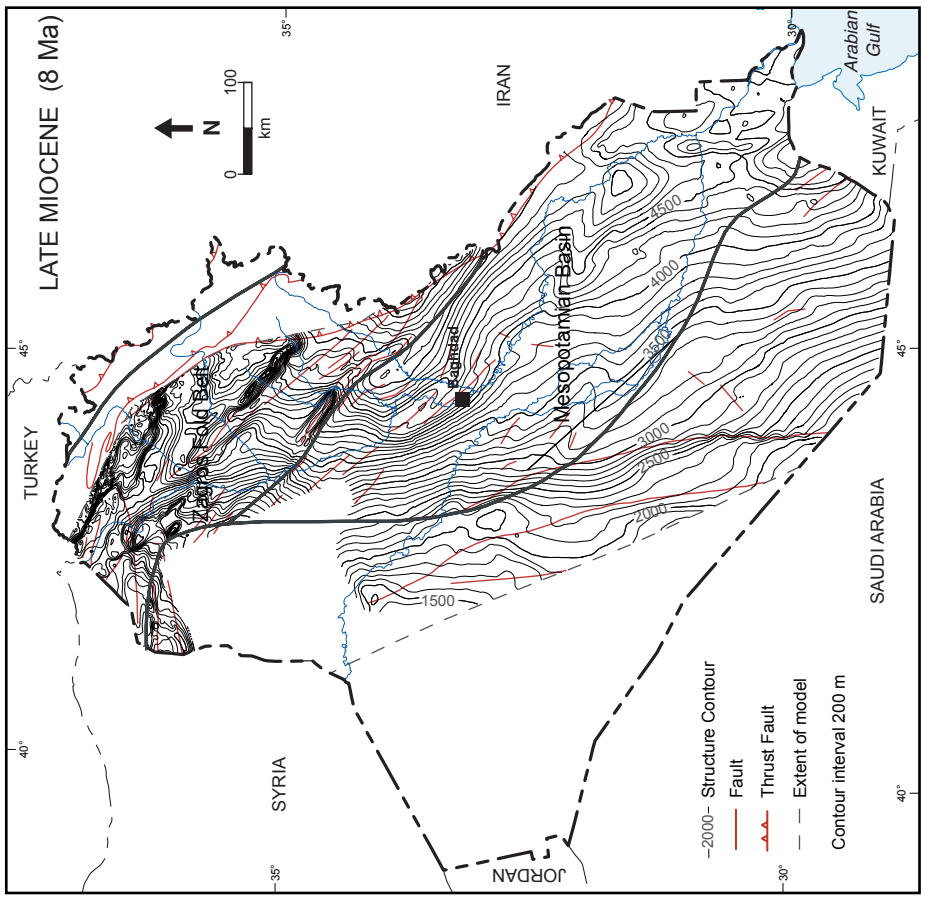
LATE MIOCENE (8 Ma)
TURKEY
SYRIA
IRAN
JORDAN
SAUDI ARABIA
KUWAIT
Arabian Gulf
Zagros Fold Belt
Mesopotamian Basin
Baghdad
N
0
100
km
1500
Structure Contour
Fault
Thrust Fault
Extent of model
Contour interval 200 m

(c)

were at maximum burial (~5,300 m) (Figure 7b). The thermal history in the northern part of the fold belt was complex during the late Cenozoic. At Baba Dome on Kirkuk anticline, for example (Figure 1), source-rock temperatures reached their peak (~130°C) at a depth of about 4,650 m in the late Miocene to early Pliocene and then decreased to their present-day value (~90°C at 3,300 m) in the late Holocene (Figure 7c). Maximum burial temperatures in synclines adjoining the Kirkuk structure also reached their highest level (~170°C) in the late Miocene. The present burial temperatures in synclines (~135°C) are approximately 35°C cooler than they were in the past.

Source Rock Maturation and Petroleum Generation

Modeled vitrinite reflectance at the top of the Middle Jurassic source-rock unit is depicted for the Mesopotamian Basin and Zagros fold belt in Figures 8a–8d. The model simulations reflect the thermal maturity (thermal stress as a function of time and temperature) that the source rocks experienced during different periods in their burial history. From the late Oligocene until the beginning of the late Miocene, high maturities (0.8–1.1% R_o) were attained locally in intrashelf basins with active source rock (Figures 8a and 8b). Deposition in these basins ceased with the onset of sedimentation in the Zagros foredeep, and rapid sediment accumulation from the late Miocene through the Pliocene led to a sharp increase in source rock maturity along the linear foredeep (Figure 8c).

At present, there is a systematic decrease in thermal maturity from east to west across the region (Figure 8d) that parallels the trend in regional structure, indicating that source rock maturation was predominantly controlled by burial. In the Mesopotamian Basin, maturities are highest, from 1.2–1.9% R_o, along the east margin where the rocks are most deeply buried and they systematically decrease updip to the west where the source-rock maturities are lowest, about 0.6% R_o. In the Zagros fold belt, source rock maturity exceeds 0.8% R_o and reaches a maximum of 1.9% R_o in the southern part. In the northern part of the fold belt, the thermal maturities generally are lower at about 0.5% R_o, although locally some maturities are as high as 1.0% R_o. East of the fold belt, in the thrust zone where the Mesozoic-Cenozoic section has undergone extensive erosion, Jurassic source rocks have exceptionally high maturity (0.92-1.95% R_o) (PGA, 2000) at or near the surface. These maturities provide evidence that uplift and exhumation took place after source-rock maturation, and they are consistent with studies that have documented an early oil phase generated and expelled in the thrust belt prior to late Cenozoic tectonism, (Dunnington, 1958). Further interpretations of the early oil phase cannot be made because the source of the oil was not determined.

Oil and gas transformation (TR) ratios and the temperatures of petroleum generation were modeled for Zubair, Kirkuk, and Khashim Ahmar fields to simulate the temperature and timing of major petroleum events (generation onset and completion), and the extent of generation at these locations (Figure 9a-9c). Vitrinite reflectance curves depicting thermal stress are shown for comparison. TR curves represent the fraction of petroleum (both oil and gas) that was generated at a given moment in geologic time. Temperatures during petroleum generation were modeled with integrated heat flow, matrix conductivity, and decompacted thickness calculations. The beginning, peak, and end of oil generation correspond to TRs of 0.01, 0.50, and 0.95, respectively, gas generated from kerogen begins and ends at TRs of 0.01 and 0.95, respectively, and oil cracking to gas starts at a TR of 0.01.

At Zubair field in the southern Mesopotamian Basin, TR and thermal curves indicate that oil generation commenced (TR > 0.01) in the Late Cretaceous at temperatures of about 80°C and reached completion (TR > 0.95) in the late Paleogene when burial temperatures were approximately 100°C, which was well before the rocks attained their maximum burial depths and temperatures (~140°C) in late Neogene. The timing of oil generation and expulsion postdated the formation of major (Paleozoic and Mesozoic) traps in the region (Figure 9a) and was highly favorable for trap charging.

The timing and extent of generation events in the Zagros fold belt are only approximate due to the complex fold geometries in the area, nevertheless insights can be gained from the transformation ratios and temperatures at key fields. At Khashim Ahmar field in the southern fold belt, the timing of oil generation was similar to that of Zubair field, with generation beginning (TR ≥ 0.01) in the Late Cretaceous and ending (TR ≥ 0.95) in the late Paleogene to early Neogene (Figure 9b). The temperatures governing generation (~70–105°C; maximum ~150°C) also were comparable to those at Zubair field (Figure 9b). Oil generated and expelled during the Late Cretaceous presumably accumulated in Cretaceous and older structural traps, whereas the later-generated oil charged Tertiary traps. In the

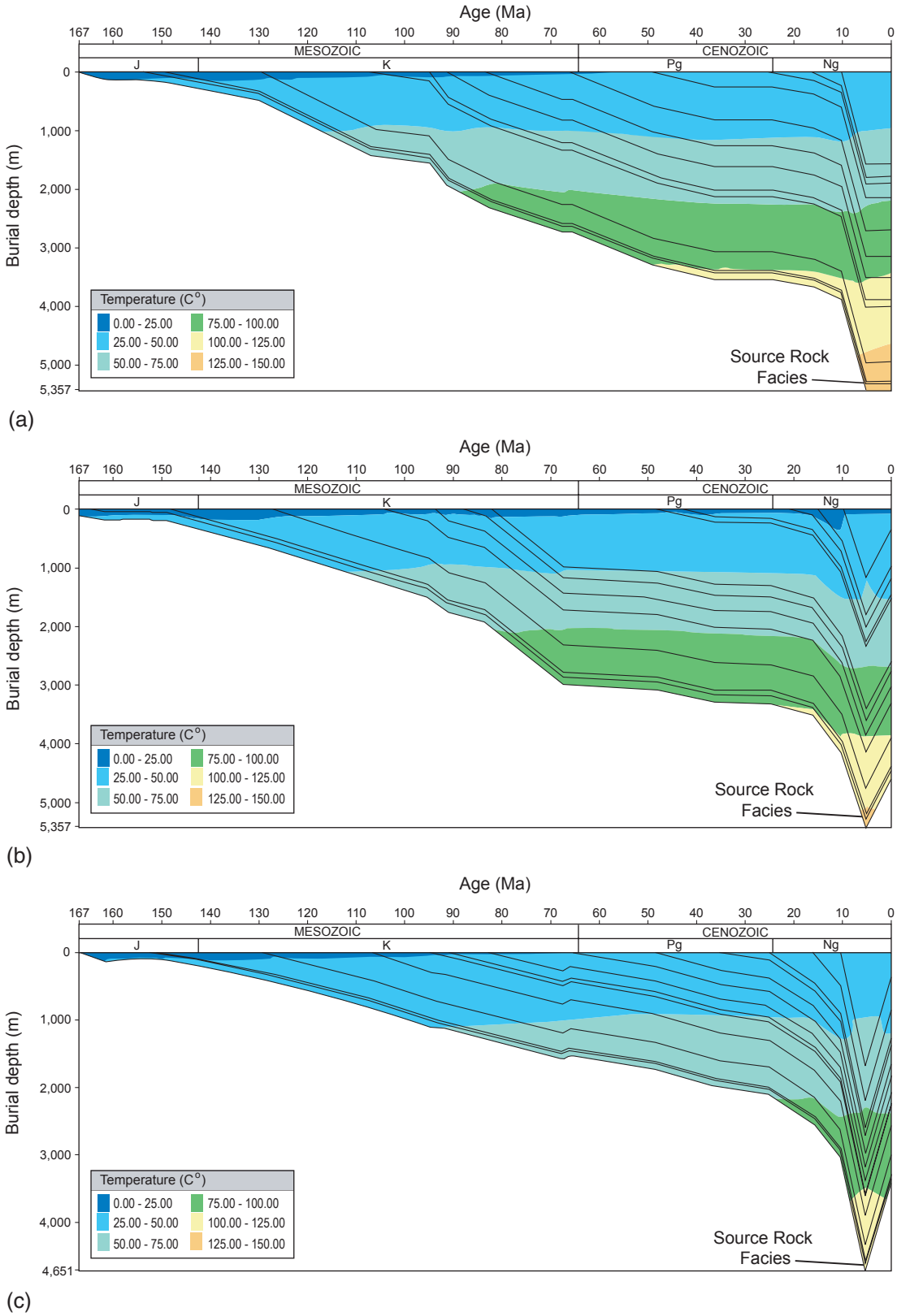

Figure 7: Burial-thermal histories of Jurassic source rocks in structures hosting: (a) Zubair field, (b) Khashim Ahmar field, and (c) Kirkuk (Baba Dome) field. See Figure 1 for field locations.

northern fold belt, oil generation and expulsion are relatively recent, and occurred within the last 8 my but the timing of generation was adverse for trap charging. At Kirkuk field on Kirkuk anticline (at Baba Dome), oil generation commenced (TR ≥ 0.01) during Paleogene-Neogene folding and faulting, and trap formation, and ceased (TR ≥ 0.95) at the onset of Holocene uplift and erosion (Figure 9c). Model

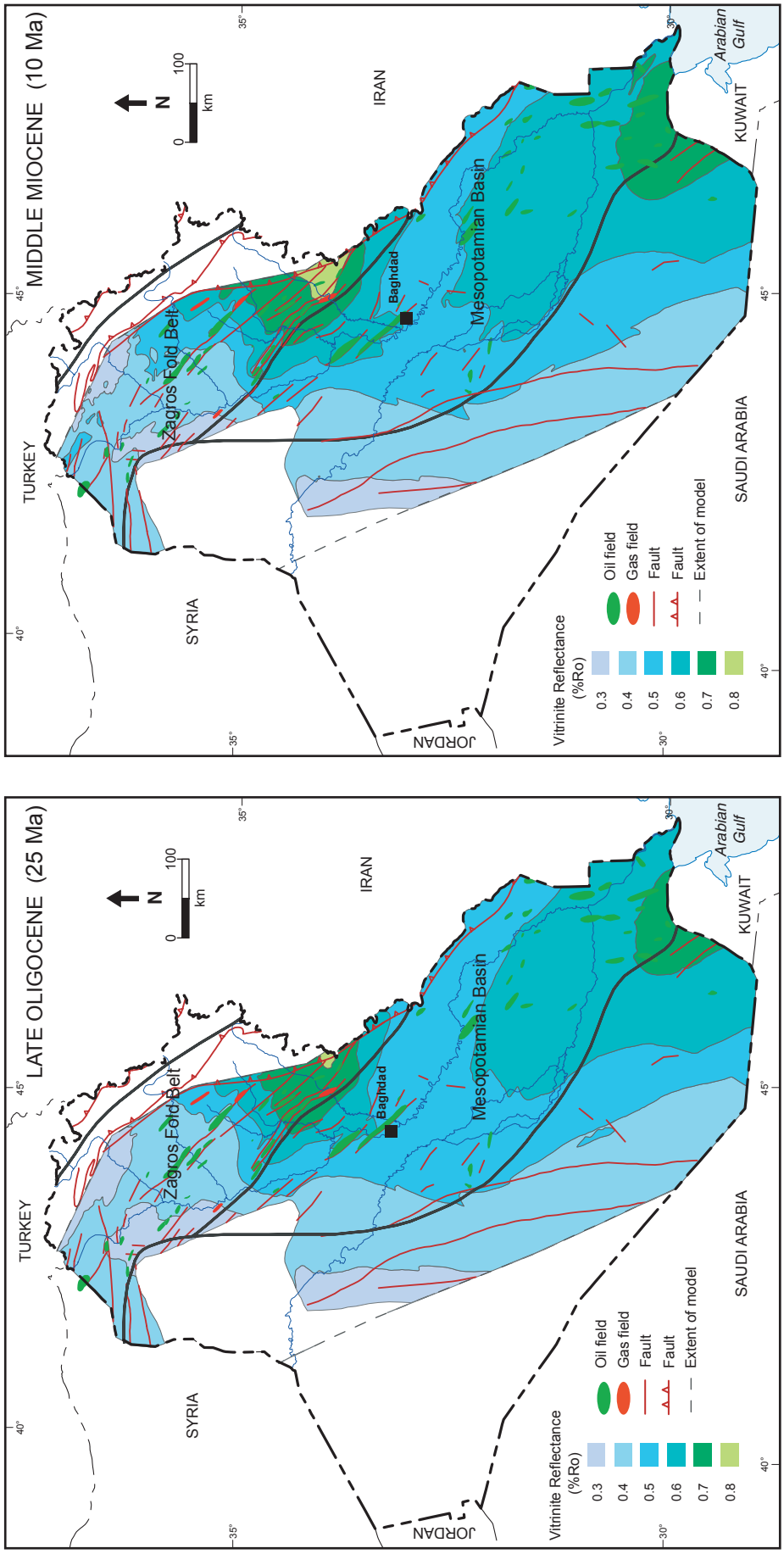

Figure 8: Modeled thermal maturity of Middle Jurassic source rocks at time periods:

(a) 25 Ma (late Oligocene), (b) 10 Ma (middle Miocene), (c) 8 Ma (late Miocene), (d) Present day.

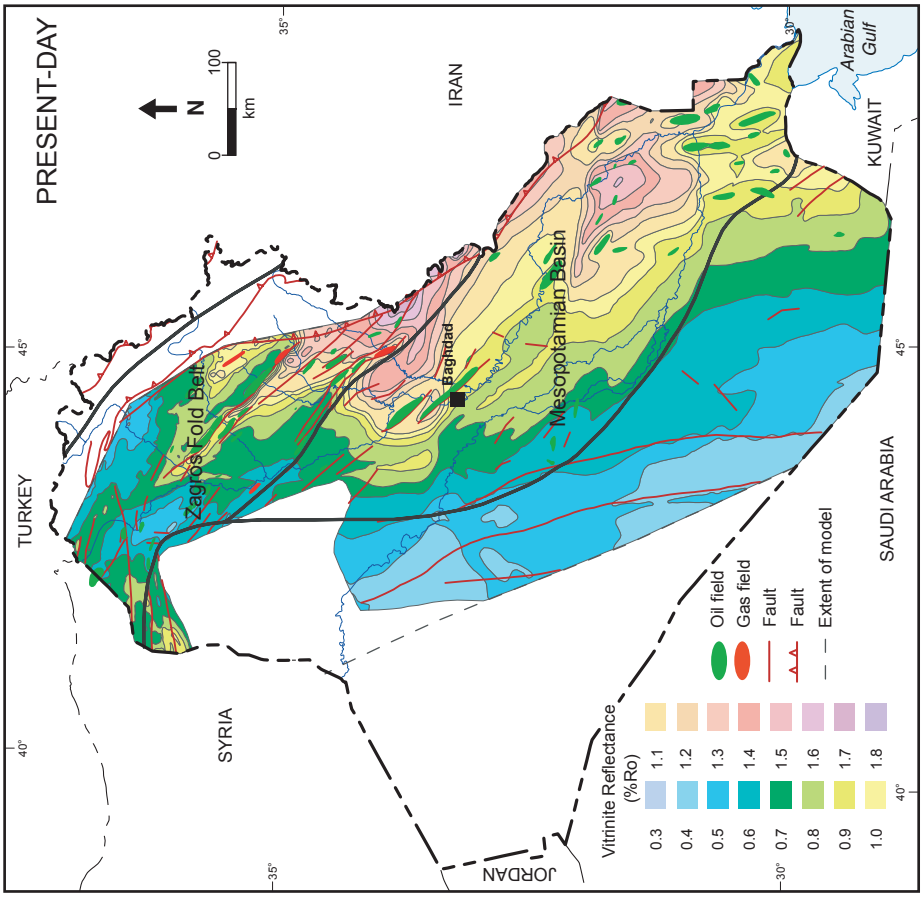
PRESENT-DAY
TURKEY
SYRIA
IRAN
JORDAN
KUWAIT
SAUDI ARABIA
Arabian Gulf
Zagros Fold Belt
Mesopotamian Basin
Baghdad
N
0
100
km
Vitrinite Reflectance (%Ro)
0.3
0.4
0.5
0.6
0.7
0.8
0.9
1.0
1.1
1.2
1.3
1.4
1.5
1.6
1.7
1.8
Oil field
Gas field
Fault
Fault
Extent of model

(d)

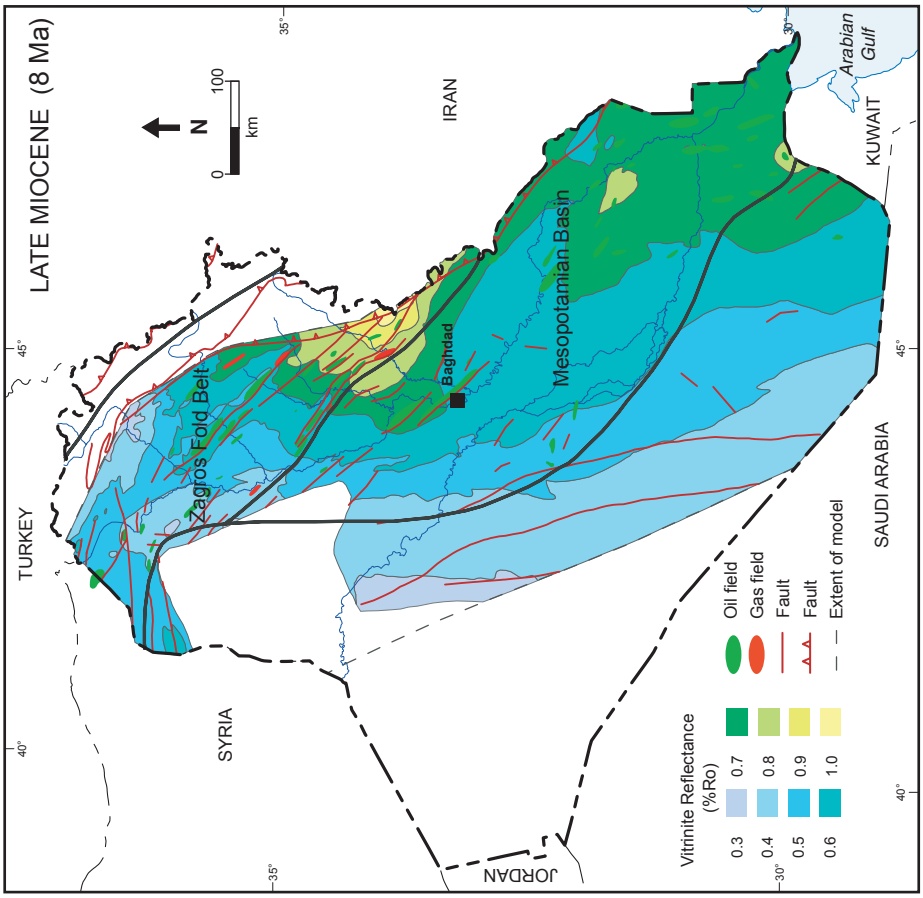
LATE MIOCENE (8 Ma)
TURKEY
SYRIA
IRAN
JORDAN
KUWAIT
SAUDI ARABIA
Arabian Gulf
Zagros Fold Belt
Mesopotamian Basin
Baghdad
N
0
100
km
Vitrinite Reflectance (%Ro)
0.3
0.4
0.5
0.6
0.7
0.8
0.9
1.0
Oil field
Gas field
Fault
Fault
Extent of model

(c)

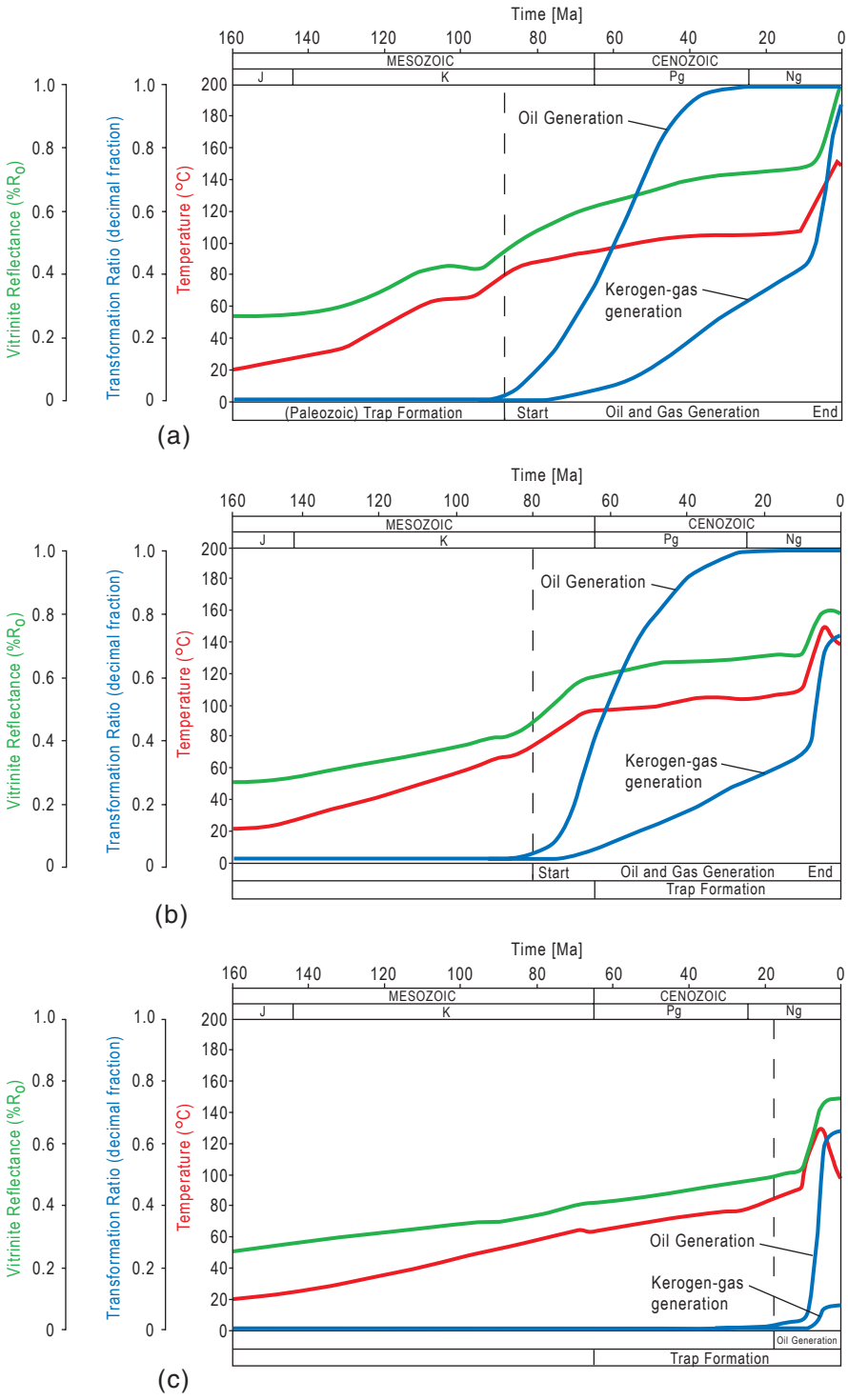

Figure 9: Oil and kerogen-gas transformation-ratio (TR) curves and thermal curves depicting timing and temperature of major petroleum-generation events, and extent of petroleum generation at: (a) Zubair field, (b) Khashim Ahmar field, and (c) Kirkuk (Baba Dome) field. Thermal maturity (R_o) curves are shown for comparison. See Figure 1 for field locations. Onset, peak, and end of oil generation correspond to a TR of 0.01, 0.50, and 0.95, respectively, and kerogen-gas generation begins and ends at a TR of 0.01 and 0.95, respectively. Petroleum event ages (dashed lines) are shown in relation to the timing of trap formation.

results indicate that source-rock temperatures at this locality increased rapidly from about 70°C at the beginning of generation to a maximum of 130°C at peak generation and then declined to approximately 90°C when generation ceased (Figure 9c).

Present oil TRs (≥ 0.95) demonstrate that virtually all Jurassic source-rock, oil-generation potential has been depleted in Zubair and Khashim Ahmar fields. At Kirkuk field (on Baba Dome), TRs of approximately 0.70 indicate that only about 70% of the oil has been generated from the source rocks. Kerogen-gas TRs for Zubair and Khashim Ahmar fields reach 0.95 and 0.70, respectively, which indicate that minor gas was generated from kerogen within the last few million years when burial temperatures had reached their peak (~140–150°C). It is significant that the maximum temperatures at these locations (~140–150°C) were not high enough to initiate oil cracking to gas in the source rock and adjacent reservoirs.

Modeled petroleum generation is depicted at a regional scale in Figures 10a–10d. Model simulations show peak oil generation (TR ≥ 0.50) active in areas (pods) of source rock in late Oligocene and middle Miocene time (Figures 10a and 10b). Beginning in the late Miocene, these areas coalesced as the foredeep filled with fine-grained sediments, and oil ultimately was generated and expelled along the entire length of the trend (Figure 10c). The area of active petroleum charge progressively deepened along the foredeep axis and expanded toward the west with increased burial from late Miocene to present-day, and, in turn, the source rocks generated most of their petroleum during this time (Figures 10c and 10d). At present, the majority of Jurassic source rocks in the Mesopotamian Basin have reached or exceeded peak oil generation (TR ≥ 0.50), and most source rocks have completed oil generation and expulsion (TR ≥ 0.95) (Figure 11d).

In the Zagros fold belt, generation ceased upon uplift and exhumation in the Holocene, but by Holocene time peak oil generation (TR ≥ 0.50) already had taken place in a large part of the region. In the southern part of the fold belt, generation has reached completion (TR ≥ 0.95) even in source rocks within a few thousand meters of the surface (Figure 10d), whereas in the northern part, a large component of the source rocks still retains more than 50% of its oil-generation potential (TR ≤ 0.50).

In the deepest parts of the Mesopotamian Basin and Zagros fold belt (east flank of foredeep), oil TRs approach 0.99, indicating that Jurassic source rocks have passed through the oil window and into the kerogen-to-gas generation zone. Modeled oil TRs of this level are supported by source-rock samples with low HI values (<70mg/g TOC) and high T_{max} values (> 450°C) from the Kirkuk 109 well (PGA, 2000) and Taq Taq 1 well (Sadooni and Alsharhan, 2003). Model simulations indicate minor gas generation from oil-prone kerogen with trace amounts of gas derived locally from the thermal cracking of oil. The transformation ratios computed for deep Jurassic source rocks (TR = 0.95–0.99) are consistent with the maximum thermal maturity modeled for the Jurassic source facies, approximately 1.9% R_o. Low gas-to-oil ratios of current proven reserves in the Mesopotamian Basin and Zagros fold belt (Verma et al., 2004) are in agreement with the model results.

Petroleum Migration and Accumulation

Secondary petroleum migration was simulated in the regional 3-D model using flow-path modeling (i.e. ray tracing). Flow-path modeling is based entirely on unit-surface geometry and does not take into account pore pressures and capillary pressures or carrier-seal relations that affect the migration system. Nevertheless, in an area of interest as large as Iraq, this method can provide valuable insights into directions of regional petroleum flow and timing of potential trap filling. Flow-path simulations typically are performed on the surfaces of carrier-beds in which reservoirs are located. In the regional 3-D model, the principal layers that focused petroleum flow are incorporated within the formations and/or groups that compose the chronostratigraphic model units, which precluded flow-path computations on individual carrier-bed surfaces. The complex facies relations (lithologic variations and unconformities) characterizing these formations and groups further complicate flow-path simulations. In the Mesopotamian Basin, Jurassic, and Cretaceous and Tertiary structure surfaces at different time periods, including present day, were geometrically very similar, thus calculated migration paths on the present Middle Jurassic surface provide a proxy for the present flow paths on the structure surfaces of Cretaceous units containing the major carrier beds. Simulated flow paths on the Middle Jurassic structure surface in the Zagros fold belt are only approximate due to the complex structure of the region; nevertheless, the flow paths are consistent with the present-day structure of the area, and thus are considered to be reasonable.

Modeled migration flow paths on the Middle Jurassic unit surface are depicted in Figures 11a-11d. Also shown are the oil and gas fields in these regions. Flow-path simulations (Figures 11a and 11b) indicate that petroleum was migrating outward from intrashelf basins owing to active source-rock generation from the late Oligocene (generation began in the Late Cretaceous) through the middle Miocene. It is

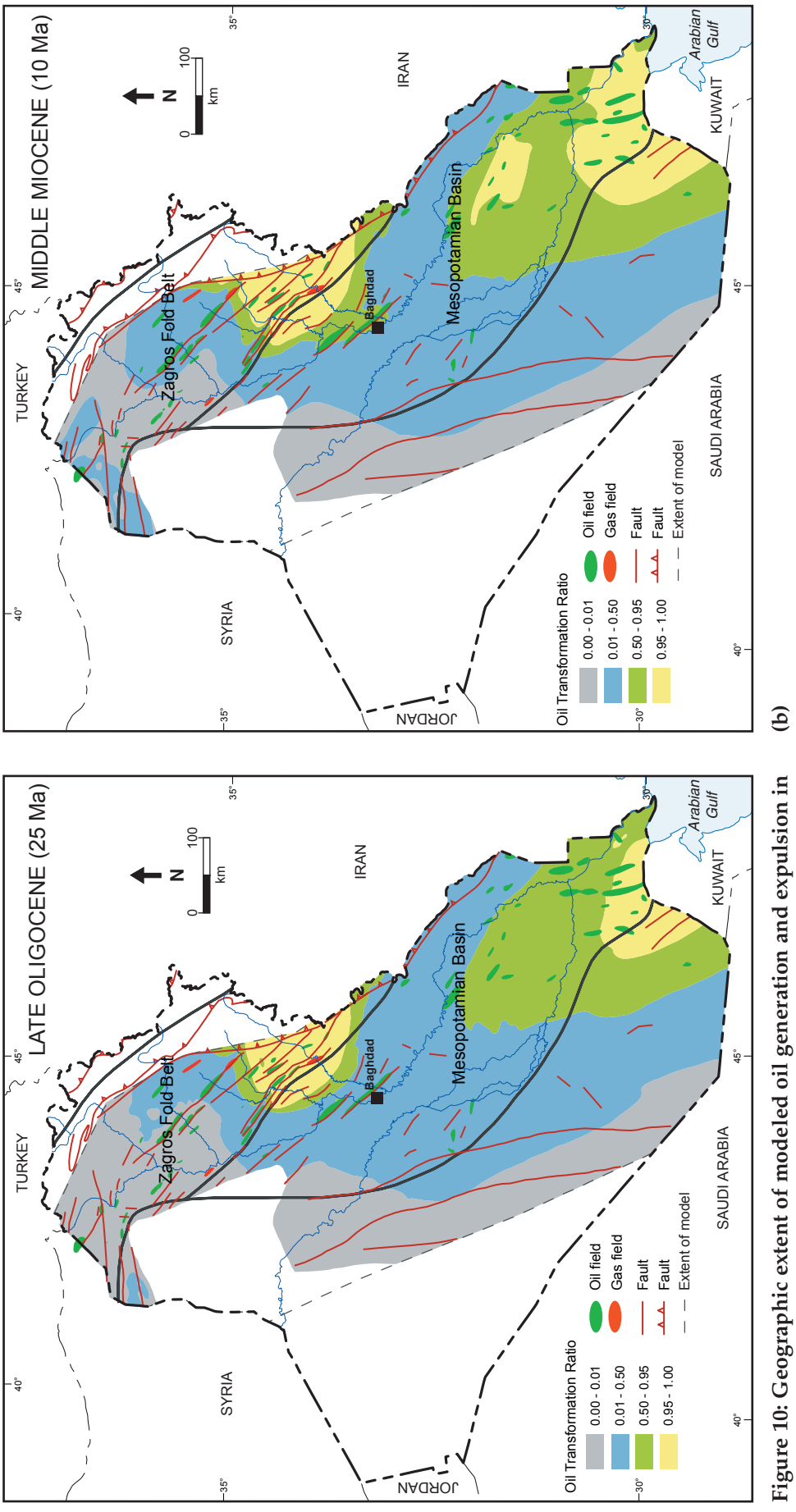

Figure 10: Geographic extent of modeled oil generation and expulsion in Middle Jurassic source rocks at time periods:

(a) 25 Ma (late Oligocene), (b) 10 Ma (middle Miocene), (c) 8 Ma (late Miocene), (d) Present day. TR contours defining end of kerogen-gas generation (TR ≥ 0.95) and onset of oil-to-gas cracking (TR ≥ 0.01) are shown for present-day.

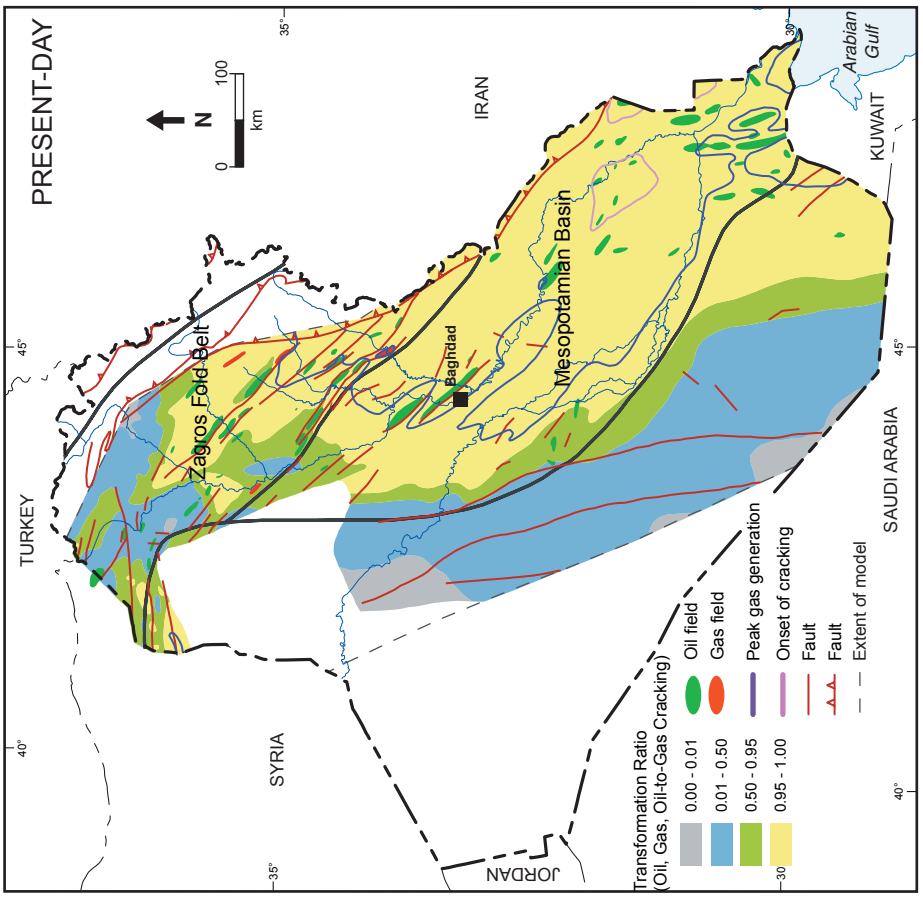
PRESENT-DAY
TURKEY
SYRIA
IRAN
JORDAN
KUWAIT
SAUDI ARABIA
Arabian Gulf
Zagros Fold Belt
Mesopotamian Basin
Baghdad
N
0
100
km
Transformation Ratio (Oil, Gas, Oil-to-Gas Cracking)
0.00 - 0.01
0.01 - 0.50
0.50 - 0.95
0.95 - 1.00
Oil field
Gas field
Peak gas generation
Onset of cracking
Fault
Fault
Extent of model

(d)

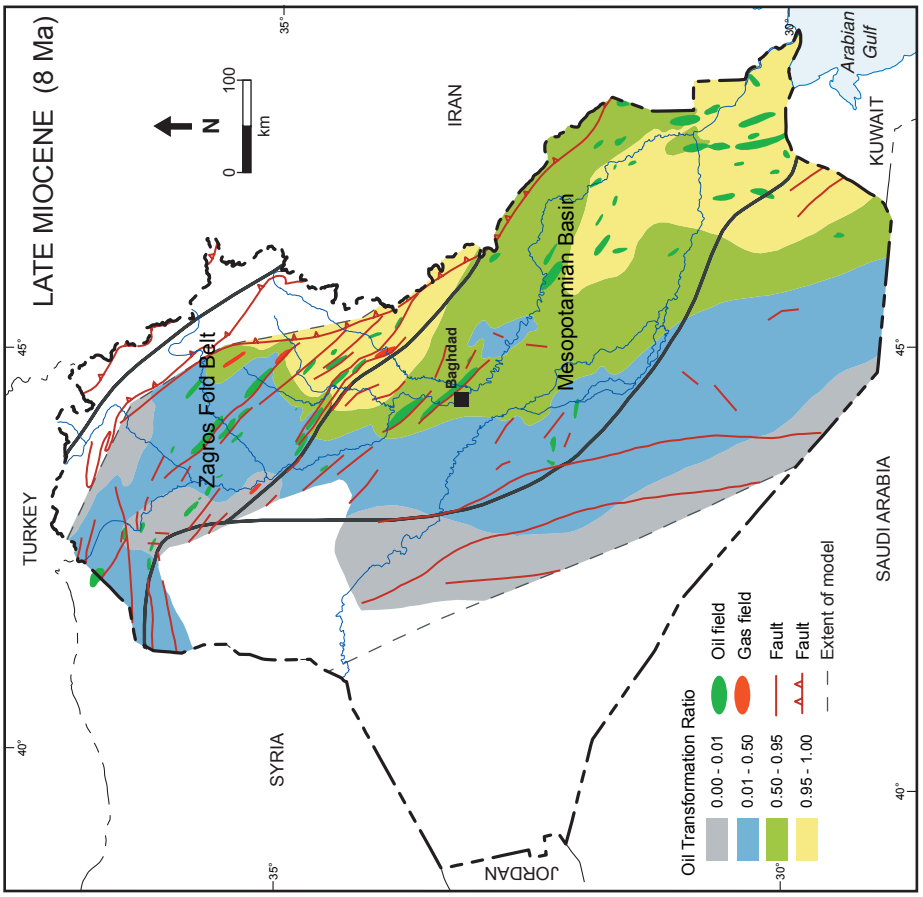
LATE MIOCENE (8 Ma)
TURKEY
SYRIA
IRAN
JORDAN
KUWAIT
SAUDI ARABIA
Arabian Gulf
Zagros Fold Belt
Mesopotamian Basin
Baghdad
N
0
100
km
Oil Transformation Ratio
0.00 - 0.01
0.01 - 0.50
0.50 - 0.95
0.95 - 1.00
Oil field
Gas field
Fault
Fault
Extent of model

(c)

noteworthy that several fields are on, or close to, the modeled migration pathways for these depocenters. Allowing for favorable trap timing, it follows that structures close to modeled flow paths within these generative areas are likely to have been charged earlier than structures situated outside these areas. In the southern intrashelf basin, the generated and expelled oil migrated and accumulated in pre-Miocene (Cretaceous and older) structures that had been affected by only minor tectonic adjustments since their inception, whereas in the fold belt in the northern intrashelf basin, oil initially migrated into (Mesozoic and Paleozoic?) structural traps that ultimately (in the late Paleogene and Neogene) were modified or destroyed. The modification and destruction of these older traps caused the oil to either remigrate into new (Tertiary) traps, or to escape from the system.

Compared to the late Oligocene and middle Miocene simulations, the migration models for the late Miocene and present-day document notably different directions and extents of petroleum flow within the region (Figure 11c and 11d). In the Mesopotamian Basin, migration from the late Miocene onward was directed to the west and southwest perpendicular to the depositional axis of the foredeep trend, whereas in the fold belt petroleum focused along northwest-trending compressional folds and fault systems. This west-northwest flow pattern reflects the shift in regional structural dip to the northeast that occurred in response to compressional tectonics and the development of the Zagros Orogen. Petroleum continued to migrate farther west through time as deposition expanded westward across eastern and central Iraq. The late Miocene flow-path model (Figure 11c) shows that the majority of fields in the Mesopotamian Basin and Zagros fold belt were located over the area of active source rock and on modeled petroleum pathways by late Miocene time, thus those fields not charged before the late Miocene received a petroleum charge during and after the late Miocene, whereas the fields that were charged earlier (from the Late Cretaceous through the middle Miocene) acquired additional charge in the late Miocene and Pliocene. In the fields that were charged earliest, the flow-path model indicates that initial petroleum generation and migration predated final entrapment by more than 60 my.

During Holocene time, continued uplift in the Zagros fold belt was accompanied by extensive erosion of reservoir and seal rocks from structural highs (2,000 m of downcutting has been estimated) and oil escaped to the surface where it accumulated locally. Modeled migration pathways presently terminate at oil seeps near the boundary of mature source rock (R_o = 0.5–0.6%) in the western part of the fold belt and in highly mature (R_o = 0.92–1.95 %) eroded outcrops of Jurassic source rock in the thrust zone (Al Mashadani, 1986; Schwartz et al., 1999; PGA, 2000) (Figure 11d). Oil accumulations also are along fault traces, indicating that additional petroleum is escaping through faults.

Flow-path modeling provides valuable information concerning the timing and directions of updip migration; however, it cannot simulate cross-formation (vertical) flow, or processes (such as pressure) controlling vertical flow. These issues were addressed in the southern Mesopotamian Basin by performing full (PVT-controlled) 3-D modeling on the petroleum drainage area containing Majnoon field (Figure 12; see inset map for location). In the area of this field, Jurassic source rocks underlie an evaporite unit (the Gotnia Formation), which separates the source (bituminous carbonate and shale) from Cretaceous reservoirs (carbonate and sandstone) (Figure 2). The drainage area in which Majnoon field is located was selected because it has its own petroleum charge (> 95% of the petroleum in the source rock has been generated and expelled) and did not receive petroleum generated from outside the area. In addition, only a minor amount of petroleum was lost from the system due to erosion or faulting. In contrast to the areal flow-path calculations, which included only the chronostratigraphic surfaces of interest, full 3-D modeling simulated the depositional and burial history of the entire stratigraphic section, including compaction, abnormal fluid pressures, multiphase (oil, gas, water) fluid flow, conductive heat flow, and kinetic reactions for petroleum generation. Simulations involving compaction and (high) pore pressures resulted in an additional driving mechanism for petroleum that could not be computed by the flow-path model.

In the 3-D area of interest (Figure 12), the model shows charged Cretaceous reservoirs in Majnoon field and in structures downdip. Petroleum in this field migrated vertically from the source through the Gotnia Formation and into the overlying E unit, where it moved along the top of the carrier bed until it reached the crest of the trapping structure. The seal efficiency of the superjacent shale relative to the oil column determined petroleum outflow through the shale into the G unit higher in the stratigraphic section. In nature, both the E unit and the G unit contain multiple accumulations. Sensitivity analysis revealed that the lithologic composition of the Gotnia Formation was a primary control on the timing and phase composition (liquid versus vapor) of the petroleum charge in Cretaceous reservoirs within these units. In the sensitivity test, end-member anhydrite and a compositional mixture (33:33:33) of anhydrite, calcite, and dolomite, respectively, were alternately assigned to the model unit containing

the Gotnia Formation. The compositional mixture was determined based on lithologic descriptions of the formation in wells west of the Majnoon structure (Ibrahim, 1978). In the model simulation where the Gotnia is defined as anhydrite, the unit acted as an effective seal due to its extremely low permeability (10^{-16} mD) and high capillary breakthrough pressure for oil (~1,600 MPa at 9% porosity), consequently petroleum migration from the source did not take place. However, in the simulation with the anhydrite-carbonate mixture, the permeability of the Gotnia unit relative to pure anhydrite was much higher (10^{-7} mD) and its sealing capacity was significantly lower (~50 MPa at 9% porosity), which permitted petroleum to move unimpeded from the source into Cretaceous reservoirs (see Figure 12). Other mechanisms (i.e., syntectonic fracturing ?) may have further modified the seal efficiency of the Gotnia, augmenting vertical petroleum flow in the drainage area.

It is significant that the simulation with the lithology mixture resulted in generated petroleum with high oil-to-gas ratios and the correct petroleum phase (oil) for each reservoir unit. The petroleum composition of the reservoirs in Majnoon field depended not only on vertical migration of oil from source rocks on structure, but also on lateral migration of oil generated off structure within permeable carrier beds. Figure 12 shows lateral petroleum flow directed updip from east to west across the drainage area; however, complex facies relations in conjunction with large trap volumes limited the extent of lateral flow to short distances, thus a vertically-drained petroleum system was dominant. It should be noted that the simulation depicted in Figure 12 does not show large amounts of oil escaping from the surface of the model, which is consistent with the absence of surface petroleum occurrences in the southern part of the Mesopotamian Basin. Results and interpretations from the model simulations can be extrapolated to other areas of the basin with similar generation histories and trapping structures.

Full-3-D modeling to assess vertical petroleum flow and trap charging was not feasible in the Zagros fold belt because structural restorations of model units, which are required to accurately reconstruct source-rock generation and migration histories, were beyond the scope of the study. Nevertheless, some general statements can be made regarding these petroleum-system processes. At present, most oil and gas fields in the fold belt overlie the modeled area of petroleum charge, which is indirect evidence that vertical migration pathways connect source rocks and reservoirs. Geologic observations (i.e. fault seeps) (Dunnington, 1958; Al Mashadani, 1986; Beydoun et al., 1992) and geochemical indicators (oil gravities, chemical compositions of oils) (Lees, 1950; Dunnington, 1958; Thode and Monster, 1970; Al Shaharistani and Al Atyia, 1972) document extensive vertical petroleum flow in the fold belt, which corroborates the model results. The majority of oil and gas fields in the Zagros fold belt are associated with steeply-dipping fault zones, or high, linear (1-10 km) structures with large-scale faults, indicating that faults were major conduits focusing petroleum flow from source to Miocene and younger traps. Seal-breach caused by tectonic-induced fracturing (Beydoun et al., 1992) facilitated additional vertical petroleum migration between reservoirs and traps. Flow-path simulations combined with results from the regional 3-D model date cross-formation flow and charging of trapping structures in the fold belt as Miocene or later.

In the eastern part of the foredeep where Jurassic source rocks have passed through the oil window ($TR \geq 0.95$) (see Figure 10d), a few structures are charged with free gas (see Figure 1 for field locations). As previously discussed, modeled temperatures during peak petroleum generation did not reach the levels required to initiate significant thermal cracking of oil, thus oil cracking within the (Jurassic) source cannot be invoked to explain the anomalous gas-to-oil ratios. In deeper (hotter), more thermally-mature rocks, a large component of gas presumably was derived from the thermal cracking of oil, assuming the source facies contained oil-prone kerogen. Thus, it is plausible that thermally-cracked gas generated at greater burial depths in the stratigraphic section on (and off) structure entered older Cretaceous reservoirs via faults and fractures displacing generated and expelled Jurassic oil into younger Tertiary traps. In the Holocene, the Tertiary traps filled with oil subsequently were truncated by erosion, leaving the deeper gas-charged reservoirs largely unaffected.

Surface oil seeps associated with faulted anticlines and breached traps in the Zagros fold belt confirm that petroleum has migrated out of the system; however, not all surface petroleum loss was related to the Zagros orogenic event (Dunnington, 1958; Beydoun et al., 1992). It should be noted that, although the regional 3-D model documents the timing of trap charging in the fold belt (within the last 8 my), it cannot account for earlier-generated petroleum (oil staining has been attributed to past oil accumulations; see Dunnington, 1958; Beydoun et al., 1992), or the trapping and remigration of petroleum from older (pre-Tertiary) structures into Tertiary reservoirs. Additional data and information are required to model processes related to these older petroleum events.

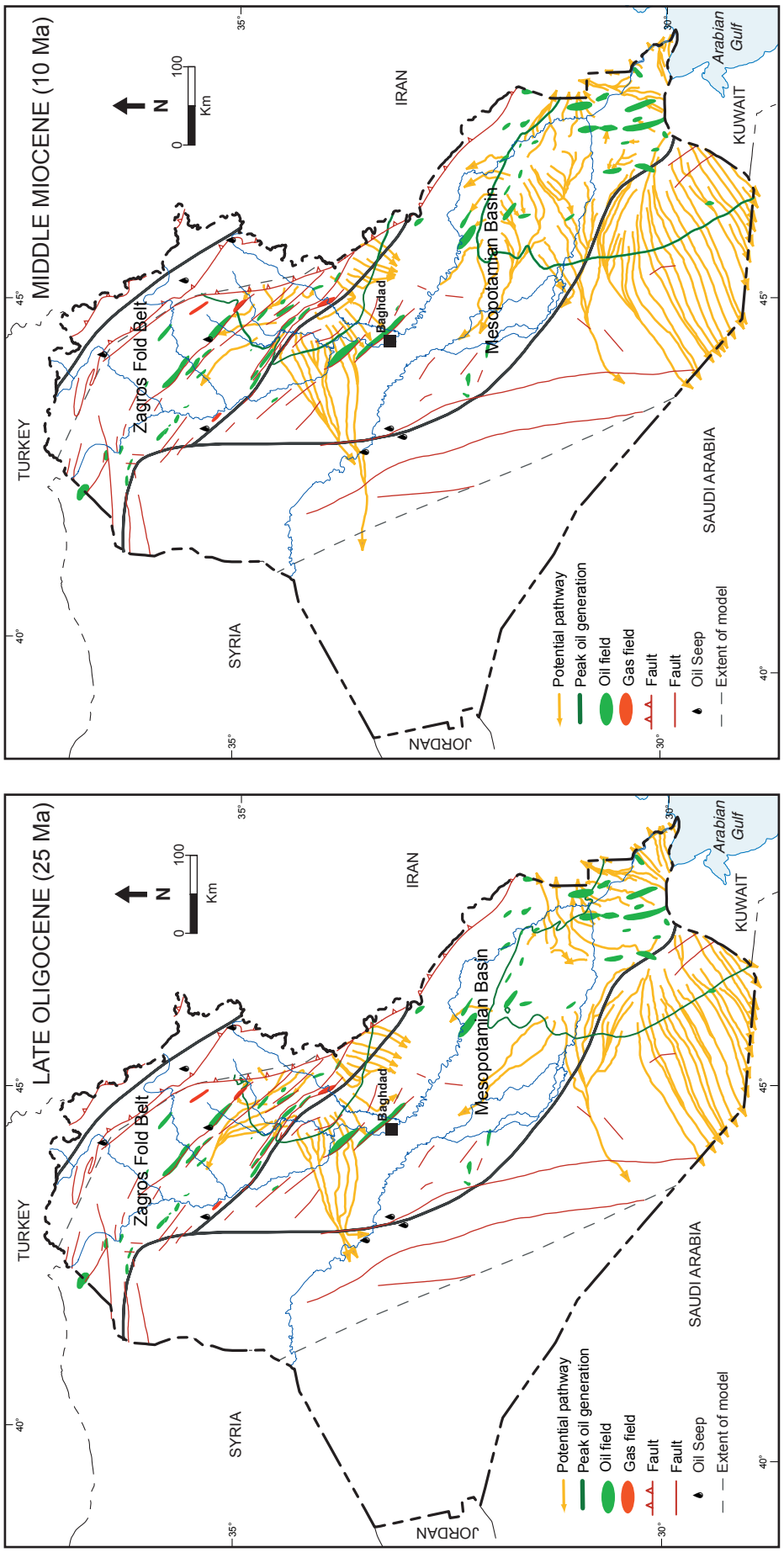

(b)

Figure 11: Modeled migration pathways on the top Middle Jurassic surface at time periods:

(a) 25 Ma (late Oligocene), (b) 10 Ma (middle Miocene), (c) 8 Ma (late Miocene), (d) Present day. TR contours depicting peak oil generation (TR ≥ 0.50) are represented for each time period. TR contours for end of kerogen-gas generation (TR ≥ 0.95) and onset of oil-to-gas cracking (TR ≥ 0.01) are shown for present-day only.

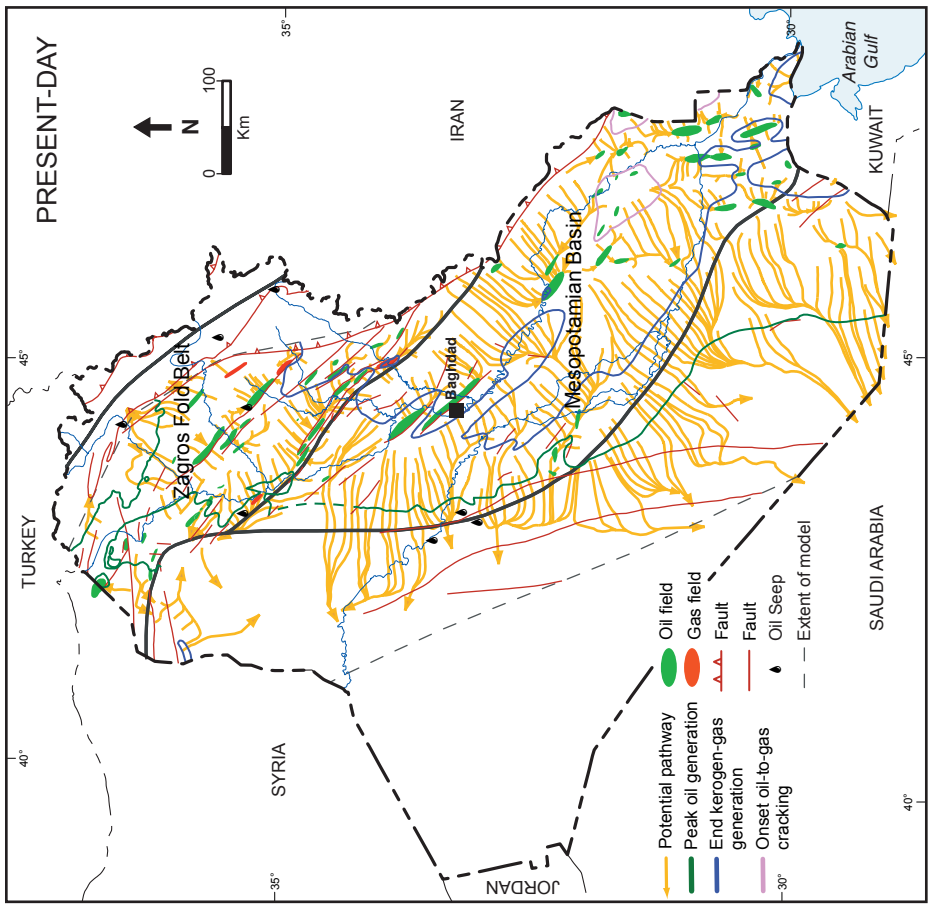
PRESENT-DAY
TURKEY
SYRIA
IRAN
KUWAIT
SAUDI ARABIA
JORDAN
Arabian Gulf
Zagros Fold Belt
Mesopotamian Basin
Baghdad
N
0
100
Km
Oil field
Gas field
Fault
Fault
Oil Seep
Extent of model
Potential pathway
Peak oil generation
End kerogen-gas generation
Onset oil-to-gas cracking

(d)

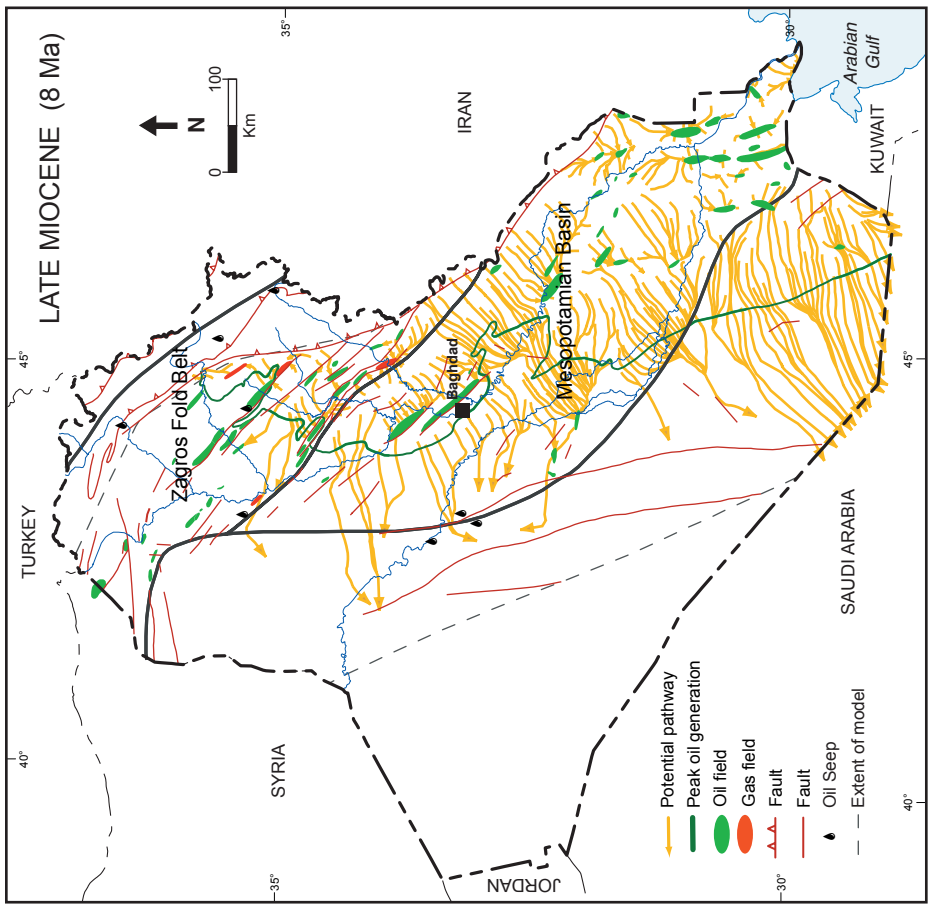
LATE MIOCENE (8 Ma)
TURKEY
SYRIA
IRAN
KUWAIT
SAUDI ARABIA
JORDAN
Arabian Gulf
Zagros Fold Belt
Mesopotamian Basin
Baghdad
N
0
100
Km
Potential pathway
Peak oil generation
Oil field
Gas field
Fault
Fault
Oil Seep
Extent of model

(c)

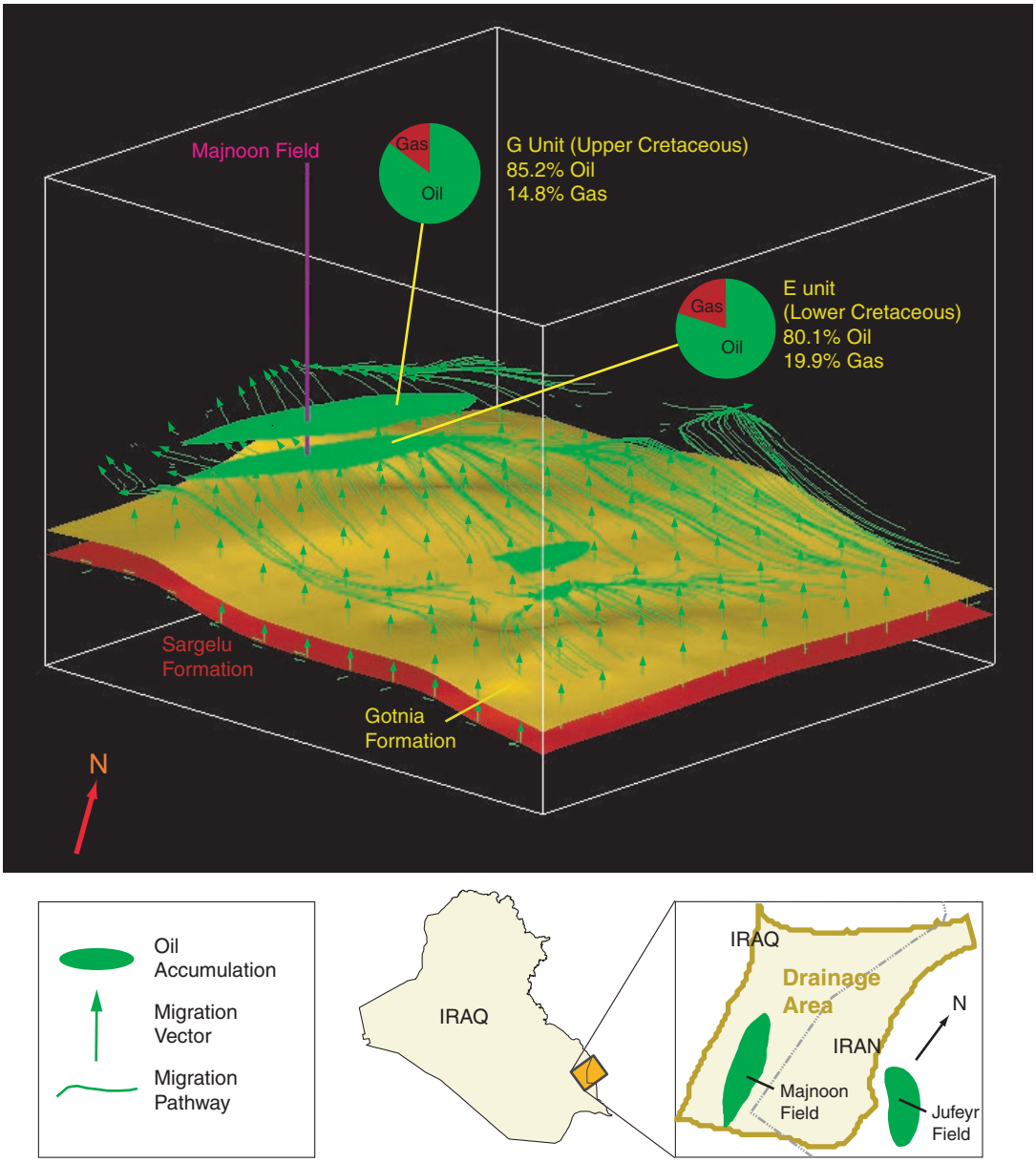

Figure 12: 3-D model simulation showing oil-flow vectors and oil accumulations for the petroleum drainage area that contains Majnoon Field. See inset maps for location of field and drainage area. 3-D modeling was performed with fully integrated pressure, volume, and temperature calculations. Color of source-rock (red) corresponds to TR ≥ 0.95.

SUMMARY

Combined thermal history and fluid-flow modeling provides an integrated analysis of the stratigraphic, thermal-maturation, and fluid-migration history of the Mesopotamian Basin and Zagros fold belt in Iraq. In this effort, we have incorporated the important aspects of the geologic and tectonic history of the region as well as the essential elements required for the generation, migration, and accumulation of petroleum into a regional 3-D model. Based on results and interpretations derived from the model simulations, some general conclusions can be made.

Organic-geochemical data indicate that the majority of the petroleum that resides in Cretaceous and Tertiary reservoirs in the Mesopotamian Basin and Zagros fold belt (TPS 203001; USGS, 2000; Verma et al., 2004) was derived from a Jurassic source. In the Mesopotamian Basin, temperatures in the Mesozoic-Cenozoic section are presently at a maximum, due to burial and subsidence that was continuous through time with little to no exhumation late in the basin's history. Jurassic source rocks in the Mesopotamian Basin are highly mature with peak oil generation and expulsion beginning in the late Paleocene. At

present, most source rocks in the Mesopotamian Basin have reached or exceeded peak oil generation (TR ≥ 0.50) and completed oil generation and expulsion (TR ≥ 0.95). Thus, the majority of the source-rock's oil-generation potential in this region has been depleted.

Thermal conditions in the present Zagros fold belt were non-uniform through time due to the combined effects of syndepositional folding and faulting related to Zagros tectonism in the late Paleogene and Neogene and extensive uplift and erosion in the Holocene. Jurassic source facies in most of the fold belt reached peak oil generation (TR ≥ 0.50) during trap formation in the late Miocene and Pliocene, before uplift and exhumation in the Holocene. Any petroleum generated and expelled prior to that time (i.e. in the latest Cretaceous) remigrated into Miocene and younger traps, or was lost from the system during late-stage uplift and unroofing. Thermal maturity modeling indicates that when generation ceased in the Holocene, peak oil generation (TR ≥ 0.50) already had occurred in a large part of the region, and locally, generation had reached completion (TR ≥ 0.95). At present, source rocks in the fold belt have expelled much of their oil (> 90%) except in the northern part where locally more than 50% of the petroleum has not been generated.

Oil and gas fields in the Mesopotamian Basin and Zagros fold belt are located over the modeled area of petroleum charge, which is consistent with a total petroleum system dominated by vertical petroleum expulsion. In the fold belt, faults were major conduits that channeled petroleum flow from source to Miocene and younger traps, and seal fracturing augmented vertical petroleum flow. Fields in close proximity to modeled migration pathways filled earliest, before the late Miocene and as early as Late Cretaceous. Beginning in the late Miocene, petroleum migration shifted from a local to a regional flow pattern in response to a northeast change in regional structural dip caused by sediment loading in the Zagros foredeep. The change in dip direction records the advance of the Zagros tectonic front and its westward expansion across eastern and central Iraq.

In the Mesopotamian Basin, migration during and after the late Miocene was directed to the west and southwest, in contrast to the fold belt where petroleum focused along northwest-trending compressional folds and fault systems. By late Miocene time, the majority of fields in the Mesopotamina Basin and Zagros fold belt were associated with active source rock and modeled petroleum pathways. Therefore, it is plausible that these fields received an initial petroleum charge during this period, or additional charge if they were filled earlier. In the fold belt, extensive exhumation of reservoir and seal rock during the Holocene (2,000 m of erosion has been estimated) led to local accumulations of surface petroleum. Oil accumulations along fault traces indicate that additional petroleum was lost through faults. Results and interpretations from early versions of the model were used in support of the USGS 2000 assessment of Iraq and to evaluate the source-rock generation potential of prospects in the Mesopotamina Basin and Zagros fold belt (Verma et al., 2004).

ACKNOWLEDGEMENTS

We sincerely thank the organizations and members of the USGS World Energy Consortium who provided encouragement for our study. We especially want to thank Mohammad Al Gailani (GeoDesign), Louis Christian (Middle East Consultant), Jim Coleman (U.S. Geological Survey, formerly with BP-Amoco), Tony Lomando (Chevron-Texaco), and Wally Pierce (Middle East Consultant, formerly with BP-Amoco) for stimulating discussions that increased our understanding of the petroleum geology of Iraq. Michael Haertle, formerly at IES, provided software support during the early stages of the study and we are grateful for his patience and assistance. The paper was reviewed by Tom Ahlbrandt, Ted Dyman, and Elisabeth Rowan of the U.S. Geological Survey, Grenville Lunn (Petroleum Geological Analysis LTD.), and by two anonymous reviewers. These individuals provided many valuable suggestions and comments and we are appreciative of their efforts. The study was conducted under the auspices of the U.S. Geological Survey World Energy Program. This report has not been reviewed for conformity with U.S. Geological Survey editorial standards or with the North American Stratigraphic Code. Final graphics ammended by *GeoArabia*.

REFERENCES

Ahlbrandt, T.S., R.M. Pollastro, T.R. Klett, C.J. Schenk, S.J. Lindquist, and J.E. Fox, 2000. Region 2 Assessment Summary—Middle East and North Africa. In USGS World Petroleum Assessment 2000—Description and Results, Chapter R2: DDS-60, 46 p.

Al Gailani, M., 2003. Assessing Iraq's oil potential. Geotimes: v. 48, p. 16-20.

Al Habba, Y.Q. and M.B. Abdullah,1989. A geochemical study of hydrocarbon source rocks in northwestern Iraq (in Arabic). Oil and Arab Cooperation Journal: v. 5T, p. 11-51.

Al Mashadani, A.A., 1986. Hydrodynamic framework of the petroleum reservoirs and cap rocks of the

Mesopotamian Basins of Iraq. Journal of Petroleum Geology: v. 9, p. 89-110.
Al Shaharistani, H. and M.J. Al Atyia, 1972. Vertical migration of oil in Iraq oil fields: evidence based on vanadium and nickel concentrations. Geochemica et Cosmochemica Acta: v. 36, p. 1303-1306.
Al Shididi, S., G. Thomas, and J. Delfaud, 1995. Sedimentology, diagenesis and oil habitat of Lower Cretaceous Qamchuqa Group, northern Iraq. American Association of Petroleum Geologists Bulletin: v. 79, p. 763-779.
Alsharhan, A.S. and A.E.M. Nairn, 1997. Sedimentary basins and petroleum geology of the Middle East. Elsevier, The Netherlands, 843 p.
Ameen, M.S., 1991. The significance of strike-slip faulting in the basement of the Zagros Fold and Thrust Belt. Journal of Petroleum Geology: v. 24, p. 5-28.
Ameen, M.S., 1992. Effects of basement tectonics on hydrocarbon generation, migration, and accumulations in northen Iraq. American Association of Petroleum Geologists Bulletin: v. 76, p. 356-370.
Aqrawi, A.A.M., 1998. Paleozoic stratigraphy and petroleum systems of the western and southwestern Deserts of Iraq. GeoArabia: v. 3, no. 2, p. 229-247.
Baskin, D.K. and K.E. Peters, 1992. Early generation characteristics of a sulfur-rich Monterey kerogen. American Association of Petroleum Geologists Bulletin: v. 76, 1-13.
Behar, F. and M. Vandenbroucke, Y. Tang, F. Marquis, and J. Espitalie, 1997. Thermal cracking of kerogen in open and closed systems: determination of kinetic parameters and stoichiometric coefficients for oil and gas generation. Organic Geochemistry: v. 26, p. 321-339.
Bellen, R.C. van, H.V. Dunnington, R. Wetzel, and D. Morton, 1959. Iraq: Lexique Stratigraphique International. Asie, Fascicle 10a, Centre National de la Recherche. Scientifique, III, Paris, 333 p.
Beydoun, Z.R., 1988. The Middle East: Regional geology and petroleum resources. Scientific Press, United Kingdom, 292 p.
Beydoun, Z.R., 1991. Arabian Plate Hydrocarbon Geology and Potential, a Plate Tectonic Approach. American Association of Petroleum Geologists Studies in Geology 33, 70 p.
Beydoun, Z.R., 1993. Evolution of the northeastern Arabian Plate margin and shelf: hydrocarbon habitat and conceptual future potential. Revue de l'Institut Francais du Petrole: v. 48, no. 4, p. 312-345.
Beydoun, Z.R., M.W. Hughes Clark, and R. Stoneley, 1992. Petroleum in the Mesopotamian Basin: A late Tertiary foreland basin overprinted onto the outer edge of a vast hydrocarbon-rich Paleozoic-Mesozoic passive-margin shelf. In R.W. Macqueen and D.A. Leckie (Eds.), Foreland Basins and Fold Belts. American Association of Petroleum Geologists Memoir 55, p. 309-339.
Bordenave, M.L. and R. Burwood, 1990. Source rock distribution and maturation in Zagros Orogenic belt: provenance of Asmari and Bangestan reservoir oil accumulations. Organic Geochemistry: v. 16, p. 369-387.
Buday, 1980. The regional geology of Iraq, Stratigraphy and paleontology. State Organization for Minerals Library, Baghdad, Iraq, v. 1, 445 p.
Burrus, J., and Audebert, F., 1990. Thermal and compaction processes in a young rifted basin containing evaporites, Gulf of Lions, France. American Association of Petroleum Geologists: v. 74, p. 1420-1440.
Christian, L., 1997. Cretaceous subsurface geology of the Middle East Region. GeoArabia: v. 2, p. 209-256.
Ditmar, V. et al. (author names not available), 1972. Geological conditions and hydrocarbon prospects of the Republic of Iraq (southern part). INOC unpublished report: INOC Library.
Dunnington, H.V., 1958. Generation, migration, accumulation and dissipation of oil in northern Iraq. In G.L. Weeks, (Ed.), Habitat of Oil. Tulsa, Oklahoma. American Association of Petroleum Geologists Bulletin: p. 1194-1251.
Gretener, P.E., 1981. Geothermics: Using temperature in hydrocarbon exploration. American Association of Petroleum Geologists Education Course Note Series 17, 170 p.
Haq, B.U., J. Hardenbol, and P.R. Vail, 1987. Chronology of fluctuating sea level since the Triassic. Science: v. 235, p. 1156-1167.
Hesp, W., and D. Rigby, 1973. The geochemical alteration of hydrocarbons in the presence of water. Erdöl und Kohle-Erdgas: v. 26, p. 70-76.
Hessami, K., H.A. Koyi, and C.J. Talbot, 2001. The significance of strike-slip faulting in the basement of the Zagros Fold and Thrust belt. Journal of Petroleum Geology: v. 24, p. 5-28.
Hooper, R.J., I.R Baron, S. Agah, and R.D. Hatcher, 1995. The Cenomanian to Recent development of the southern Tethyan margin in Iran. In M.I. Al-Husseini (Ed.), Middle East Petroleum Geosciences, Geo'94. Gulf PetroLink, Bahrain, v. 2, p. 505-516.
Hunt, J. M., M. D. Lewan, and J.C. Hennet, 1991. Modeling oil generation with time-temperature index graphs based on the Arrhenius equation. American Association of Petroleum Geologists Bulletin: v. 75, p. 795-807.
Ibrahim, M.W., 1978. Petroleum Geology of southern Iraq. PhD Thesis, Imperial College, University of London, 479 p.
Ibrahim, M.W., 1983. Petroleum geology of southern Iraq. American Association of Petroleum Geologists Bulletin: v. 67, p. 97-130.
Ibrahim, M.W., 1984. Geothermal gradient and geothermal oil generation in southern Iraq: A

preliminary investigation. Journal of Petroleum Geology: v.7, p. 77-86.
IHS Energy Group (formerly Petrolconsultants), 1981, 1986, 1991, 1996. International Petroleum Exploration and Production Database. Database available from IHS Energy Group, 15 Inverness Way East, Englewood, CO, 80112, U.S.A..
IES Integrated Exploration Systems, 2004. PetroMod, 1D/PetroCharge Express, and PetroRisk Software. IES, Bastionstrasse 11-19, 52428 Juelich, Germany, (www.ies.de).
Jackson, J.A. and D.P. McKenzie, 1984. Active tectonics of the Alpine-Himalayan belt between western Turkey and Pakistan. Geophysical Journal of the Royal Astronomical Society: v. 77, p. 185-264.
Knauss, K.G., S.A Copenhaver, R.L. Braun, and A.K. Burnham, 1997. Hydrous pyrolysis of New Albany and Phosphoria shales: Production kinetics of carboxylic acids and light hydrocarbons and interactions between the inorganic and organic chemical systems. Organic Geochemistry: v. 27, p. 477-496.
Lee, W.H.K., and S. Uyeda, 1965. Review of heat flow data. In W.H.K. Lee (Ed.): Terrestrial Heat Flow. American Geophysical Union Monograph 8, p. 87-190.
Lees, G.M., 1950. Some structural and stratigraphical aspects of the oil fields of the Middle East. Report of the 18th International Geological Congress, Great Britian, 1948, v. 6, p.26-33.
Lewan, M. D., 1985. Evaluation of petroleum generation by hydrous pyrolysis experimentation. Philosophical Transactions of the Royal Society of London, Series A, v. 315, no. 1531, p. 123-134.
Lewan, M. D., 1998. Sulfur radical control on petroleum formation rates. Nature: v. 391, no. 8, p. 164-166.
Lewan, M. D. and A. A. Henry, 2001. Gas:oil ratios for source rocks containing Type-I, -II, -IIS, and –III kerogens as determined by hydrous pyrolysis. In T. Dyman and V. Kuuskraa, (Eds.), Geological studies of deep natural gas resources: U.S. Geological Survey DDS-67, Chapter E, CD-ROM.
Lewan, M. D. and T.E. Ruble, 2002. Comparison of petroleum generation kinetics by isothermal hydrous and nonisothermal open-system pyrolysis. Organic Geochemistry: v. 33, p. 1457-1475.
Murris, R. J., 1980. Middle East: Stratigraphic evolution and oil habitat. American Association of Petroleum Geologists Bulletin: v. 64, p. 597-618.
Orr, W. L., 1986. Kerogen/asphaltene/sulfur relationships in sulfur-rich Monterey oils. Organic Geochemistry: v. 10, p. 499-516.
Orr, W. L., 2001. Evaluating kerogen sulfur content from crude oil properties. In C. M. Isaacs, and J. Rullkotter (Eds.), The Monterey Formation from Rocks to Molecules. Columbia University Press, New York, p. 348-367.
Orr, W. L. and J. S. Sinninghe Damsté, 1990. Geochemistry of sulfur in petroleum systems. In W. L. Orr and C. M. White (Eds.), Geochemistry of Sulfur in Fossil Fuels: ACS Symposium Series 429, Chapter 1. Washington, DC, p. 2-29.
Petersen, N. F. and P. J. Hickey, 1987. California Plio-Miocene oils: Evidence of early generation. In R. E. Meyer (Ed.), American Association of Petroleum Geologists, Studies in Geology No. 25, Exploration for Heavy Oil and Natural Bitumen, p. 351-359.
PGA (Petroleum Geological Analysis LTD.), 2000. Source rock potential and maturity of the Sargelu and Naokelekan Formations in Iraq. Database available from Petroleum Geological Analysis LTD., Quantock and Saker Geological Services, University of Reading, 69 High Street West Glossop, Derbyshire SK138AZ, England (www.pgal.co.uk).
Price, L.C., 1997. Minimum thermal stability levels and controlling parameters of methane, as determined by C_{15+} hydrocarbon thermal stability. U. S. Geological Survey Bulletin 2146-K, p. 135-176.
Sadooni, F.N., 1997. Stratigraphy and petroleum prospects of Upper Jurassic carbonates in Iraq. Petroleum Geoscience: v. 3, p. 233-243.
Sadooni, F.N. and A.A.M. Aqrawi, 2000. Cretaceous sequence stratigraphy and petroleum potential of the Mesopotamian Basin, Iraq. In Middle East Models of Jurassic/Cretaceous Carbonate Systems, SEPM Special Publication No. 69, p. 315-334.
Sadooni, F.N. and A.S. Alsharhan, 2003. Stratigraphy, microfacies, and petroleum potential of the Mauddud Formation (Albian-Cenomanian) in the Arabian Gulf Basin. American Association of Petroleum Geologists Bulletin: v. 87, p. 1653-1680.
Schwartz, M., D. Hollander, and G. Stein, 1999. Reconstructing Mesopotamian exchange networks in 4th Millenium BC: Geochemical and archeological analyses of bitumen artifacts from Hacinebe Tepe, Turkey. Paleorient: v. 15, p 67-82.
Sharland, P.R., R. Archer, D.M. Casey, R.B. Davies, S.H. Hall, A.P. Heward, A.D. Horbury, and M.D. Simmons, 2001. Arabian Plate Sequence Stratigraphy. GeoArabia Special Publication 2, Gulf Petrolink, Bahrain, 371 p.
Stoneley, R., 1987. A Review of petroleum source rocks in parts of the Middle East. In J. Brooks and A.J. Fleet, (Eds.), Marine Petroleum Source Rocks: The Geological society (London) Special Publication 26, p. 263-269.
Stoneley, R., 1990. The Middle East Basin: A summary overview. In J. Brooks (Ed.), Classic Petroleum Provinces: Geological Society Special Publications 50, p. 293-298.
Sweeney, J.J. and A.K. Burnham, 1990. Evaluation of a simple model of vitrinite reflectance based on chemical kinetics. American Association of Petroleum Geologists Bulletin: v. 74, p. 1559-1570.

Tannenbaum, E. and Z. Aizenshtat, 1985. Formation of immature asphalt from organic-rich carbonate rocks-I. Geochemical correlation. Organic Geochemistry: v. 8, p. 181-192.

Thode, H.G. and J. Monster, 1970. Sulfur isotope abundance and generic relations of oil accumulations in Middle East Basin. American Association of Petroleum Geologists Bulletin: v. 54, p. 627-637.

Tissot, B.P., R. Pelet, and P. Ungerer, 1987. Thermal history of sedimentary basins, maturation indices, and kinetics of oil and gas generation. American Association of Petroleum Geologists Bulletin: v. 71, p. 1445-1466.

Tomic, J., F. Behar, M. Vandenbroucke, and Y. Tang, 1995. Artificial maturation of Monterey kerogen (Type II-S) in a closed system and comparison with Type II kerogen: Implications on the fate of sulfur. Organic Geochemistry: v. 23, p. 647-660.

Tsuzuki, N., N. Takeda, M. Susuki, and K. Yokoi, 1999. The kinetic modeling of oil cracking by hydrothermal pyrolysis experiments. International Journal of Coal Geology: v. 39, p. 227-250.

U.S. Geological Survey World Petroleum Assessment 2000-Description and Results: U.S. Geological Survey Digital Data Series DDS-60, version 1.1, four CD-ROM set.

Verma, M.K., T.S. Ahlbrandt, and M. Al Gailani, 2004. Petroleum reserves and undiscovered resources in the Total Petroleum Systems of Iraq: Reserve growth and production implications. GeoArabia: v. 9, No. 3, p. 51-74.

ABOUT THE AUTHORS

Janet K. Pitman *is a Research Petroleum Geologist in the Central Energy Team at the United States Geological Survey. Her current research focuses on reservoir characterization, petroleum system modeling, and basin analysis in support of USGS domestic and world energy resource assessments. Since 1995 Janet has worked in cratonic basins of the US MidContinent, the Northern Rocky Mountains, and the onshore Gulf Coast as well as the Middle East and Arctic. She is a member of the American Association of Petroleum Geologists and the Society of Sedimentary Geology. Janet attended the University of Colorado and the Colorado School of Mines.*

jpitman@usgs.gov

Douglas W. Steinshouer *joined the United States Geological Survey Central Energy Team as a Consulting GIS Analyst in 1997. He provides GIS and cartographic support to the USGS World Petroleum Assessment 2000, as well as participating in the compilation of digital geological maps of the Former Soviet Union, the Asia-Pacific Region, Europe and Iran. Douglas also has provided data preparation and computer support to basin modeling efforts in the US Gulf Coast, Canada's Beaufort Sea-Mackenzie Delta and the Middle East.*

steinsho@usgs.gov

Michael D. Lewan *has been employed as an organic geochemist for the Central Energy Resources Team of the US Geological Survey since 1991. His prior experience includes 13 years as a research geochemist with Amoco Production Company and 3 years as an exploration geologist with Shell Oil Company. He received his PhD from the University of Cincinnati, MS from Michigan Technology University, and BS from Northern Illinois University. Mike's research interests involve laboratory simulation of natural petroleum formation for the evaluation of expulsion efficiencies, kinetic parameters, and petroleum potential of source rocks. Since 1995 he has conducted petroleum source-rock studies in Rocky Mountain Basins, the onshore Gulf Coast, Polish Carpathians, US Mid-Continent, and the Middle East. He is a member of the American Association of Petroleum Geologists, Geochemical Society, Geological Society of America, The Society for Organic Petrology, and American Association for the Advancement of Science.*

mlewan@usgs.gov

Manuscript Received May 5, 2004

Manuscript Revised July 1, 2004

manuscript Accepted July 5, 2004

Press Version Proofread by Authors August 18, 2004